



KTH Electrical Engineering

**Partial Discharge Signatures of Defects in Insulation Systems  
Consisting of Oil and Oil-impregnated Paper**

MOHAMAD GHAFARIAN NIASAR

Licentiate Thesis

Stockholm, Sweden 2012

Division of Electromagnetic Engineering

KTH School of Electrical Engineering

SE- 100 44 Stockholm, Sweden

TRITA-EE 2012:059

ISSN 1653-5146

ISBN 978-91-7501-573-6

Akademisk avhandling som med tillstånd av Kungl Tekniska högskolan framlägges till offentlig granskning för avläggande av teknologie licentiatexamen fredagen den 7 december 2012 klockan 13.00 i H21, Teknikringen 33, 1 tr, Kungl Tekniska högskolan, Stockholm.

© Mohamad Ghaffarian Niasar, December 2012

Tryck: Universitetsservice US AB

## **Abstract**

Partial discharge measurement is a common method for monitoring and diagnostics of power transformers, and can detect insulation malfunctions before they lead to failure. Different parameters extracted from the measured PD activity can be correlated to the PD source, and as a result it is possible to identify the PD source by analyzing the PD activity.

In this thesis, possible defects that could cause harmful PDs in transformers were investigated. These defects include corona in oil, a void in pressboard, a metal object at floating potential, surface discharge in oil, a free bubble in oil and small free metallic particles in oil. The characteristics of disturbing discharge sources were analyzed, like corona in air, surface discharge in air, and discharge from an unearthed object near to the test setup.

The PD activity was recorded both in the time domain and phase domain, and possible characteristics for each PD pattern and waveform were extracted in order to find the best characteristic for the purpose of classification.

The results show that in the phase domain parameters such as phase of occurrence, repetition rate and shape of PD pattern are most suitable for classification while magnitude of discharge can only be useful in specific cases. The results show that the PD waveforms correlated to different defects are similar; however the time domain data include all the information from the phase domain, and also has the potential to identify the number of PD sources.

The PD dependency on temperature was investigated on the four test objects including surface discharges in oil, corona in oil, bubble discharges in oil, and metal object at floating potential. The effect of humidity was investigated for corona in oil. The results show that at higher temperature the corona activity in oil and PD activity due to a metal object at floating potential in oil decrease. However, for a bubble in oil and for surface discharge in oil the PD activity increases with the increase of the oil temperature. It was shown that the amount of moisture in oil has a strong impact on number of corona pulses in oil.

The last part focused on ageing of oil-impregnated paper due to PD activity. Investigation was made of the behavior of PD activity and its corresponding parameters such as PD repetition rate and magnitude, from inception until complete puncture breakdown. The results show that both the number and magnitude of PD

increase over time until they reach to a peak value. After this point over time both curves decrease slowly, and eventually full breakdown occurs.

The effect of thermal ageing of oil impregnated paper on time to breakdown and PD parameters was investigated. The results show that thermal aging of oil-impregnated paper increases the number and magnitude of PD. Dielectric spectroscopy was performed on the samples before and after PD ageing and the result was used in order to explain the behavior of PD over time.

## **Acknowledgements**

I would like to thank my supervisor Associate professor Hans Edin for his guidance in this project. Productive discussions and comments received from him have shown me the right way. My special thanks go to Dr. Nathaniel Taylor for assistance with laboratory equipment. I also like to thank Prof. Rajeev Thottappillil, head of the department, for all his efforts to make the department a nice place to work.

Dr. Demetres Evagorou recently started his post-doctoral studies in our group. I would like to thank him for his comments on this thesis.

I am very grateful to my friends in the high-voltage research group, Tech. Lic. Nadja Jäverberg, Xiaolei Wang, Respicius Clemence, Håkan Westerlund and Roya Nikjoo for creating a very friendly atmosphere to work in.

Thanks to the all colleagues in Teknikringen 33 especially to my Persian friends Seyed Ali Mousavi and Hanif Tavakoli and my ‘room sharer’ Johanna Rosenlind for having a lot of fun discussions.

Also I would like to thank our financial administrator Ms. Carin Norberg and system administrator Mr. Peter Lönn, and workshop responsible Mr. Jesper Freiberg for making some of my experimental test cells.

I would like to thank ABB for supplying paper and pressboard, Nynas-AB for supplying transformer oil and Vattenfall/Forsmark nuclear power station for supplying an aged transformer bushing.

The project was funded by the Swedish center of Excellence in Electric Power Engineering – EKC<sup>2</sup> which is greatly acknowledged. The project is also part of KIC-InnoEnergy through the CIPOWER innovation project.

Last but not least I would like to thank my family for their great support during my study. Thanks to my father for his encouragement, thanks to my mother for her love to me and thanks to my sisters and brothers for their support during my educational career.

*Mohamad Ghaffarian Niasar*  
*Stockholm, December 2012*



## List of Papers

This work is based on following papers:

- I. **M. Ghaffarian Niasar**, H. Edin, “Corona in Oil as a Function of Geometry, Temperature and Humidity” Conference on Electrical Insulation and Dielectric Phenomena (CEIDP), October 2010, West Lafayette, USA.
- II. **M. Ghaffarian Niasar**, H. Edin, “Partial Discharge Due to Bubbles in Oil” Nordic Insulation Symposium, June 2011, Tampere, Finland.
- III. **M. Ghaffarian Niasar**, H. Edin, X. Wang and R. Clemence, “Partial Discharge Characteristics Due to Air and Water Vapor Bubbles in Oil” 17<sup>th</sup> International Symposium on High Voltage Engineering, August 22<sup>nd</sup>-26<sup>th</sup> 2011, Hannover, Germany.
- IV. **M. Ghaffarian Niasar**, R. Clemence, X. Wang, R. Nikjoo, H. Edin, “Effect of Temperature on Surface Discharge in Oil” IEEE Conference on Electrical Insulation and Dielectric Phenomena (CEIDP), October 2012, Montreal, Canada.
- V. R. Clemence Kiiza, **M. Ghaffarian Niasar**, R. Nikjoo, X. Wang and H. Edin, “Partial Discharge Patterns in a Cavity Embedded in Oil-Impregnated Papers, Part 1 – Effect of High Voltage Impulses”, submitted to IEEE Transactions on Dielectrics and Electrical Insulation.
- VI. **M. Ghaffarian Niasar**, R. Clemence Kiiza, X. Wang, Hans Edin, “Partial Discharge Patterns in a Cavity Embedded in Oil-Impregnated Papers, Part 2 – Effect of Thermal Ageing and Partial Discharge Deterioration”, submitted to IEEE Transactions on Dielectrics and Electrical Insulation.

The author has also contributed to the following papers, but they are not included in this thesis.

- VII. R. Clemence Kiiza, **M. Ghaffarian Niasar**, R. Nikjoo, X. Wang and H. Edin, “Comparison of Phase Resolved Partial Discharge Patterns in Small Test Samples, Bushing Specimen and Aged Transformer Bushing” IEEE Conference

on Electrical Insulation and Dielectric Phenomena (CEIDP), October 2012, Montreal, Canada.

- VIII. R. Clemence Kiiza, R. Nikjoo, **M. Ghaffarian Niasar**, X. Wang and H. Edin, “Effect of High Voltage Impulses on Partial Discharge Activity in a Cavity Embedded in Paper Insulation” IEEE Conference on Electrical Insulation and Dielectric Phenomena (CEIDP), October 2012, Montreal, Canada.
- IX. X. Wang, **M. Ghaffarian Niasar**, R. Clemence, H. Edin, “Partial Discharge Analysis in a Needle-plane gap with Repetitive Step Voltage” IEEE Conference on Electrical Insulation and Dielectric Phenomena (CEIDP), October 2012, Montreal, Canada.
- X. R. Nikjoo, N.Taylor, **M. Ghaffarian Niasar**, H. Edin, “Dielectric Response Measurement of Power Transformer Bushing by utilizing High Voltage Transients” IEEE Conference on Electrical Insulation and Dielectric Phenomena (CEIDP), October 2012, Montreal, Canada.



# Contents

<b>1</b>	<b>Introduction</b> .....	1
1.1	Background .....	1
1.2	Literature review .....	4
1.3	Aim.....	8
1.4	Thesis outline .....	8
1.5	Author’s contributions .....	9
<b>2</b>	<b>PD basics, equivalent circuit and detection methods</b> .....	11
2.1	Types of partial discharges .....	11
2.2	PD equivalent circuit .....	14
2.3	PD detection and localization.....	16
<b>3</b>	<b>Measurement systems</b> .....	21
3.1	PD measurement system .....	21
3.2	Dielectric spectroscopy measurement in frequency domain.....	24
3.3	Polarization and depolarization current measurement .....	25
<b>4</b>	<b>Partial discharge classification</b> .....	27
4.1	Formats of data saving .....	27
4.2	PDs on the insulating system consisting of oil and oil-impregnated paper .....	30
4.3	Phase domain and Time domain characteristics.....	30
4.4	PD measurement on a 36 kV bushing .....	38
<b>5</b>	<b>Disturbing sources of PD</b> .....	43
5.1	Corona in air .....	43
5.2	Surface discharge in air .....	45
5.3	Unearthed metal object near to experiment .....	46
5.4	Ungrounded bushings tap .....	47

<b>6</b>	<b>Effect of temperature on partial discharge .....</b>	<b>49</b>
<b>7</b>	<b>Deterioration of oil-impregnated paper due to PD activity .....</b>	<b>53</b>
<b>8</b>	<b>Summary of papers .....</b>	<b>57</b>
<b>9</b>	<b>Conclusions and future work .....</b>	<b>61</b>
	<b>Bibliography .....</b>	<b>63</b>
	<b>Papers I-VI.....</b>	<b>68</b>

# Chapter 1

## Introduction

### 1.1 Background

The power transformer is used to convert between different voltage levels and is one of the most critical components of a power system. The power transformer itself is very expensive, but since the repair-time for a power transformer may be several months, the cost of unavailability is also significant. Many transformers in the world have today reached their design lifetime but are still in operation, and it has a strong economic impact if they can continue to run safely over many years. The repair or replacement cost of a transformer, together with the possibility of undelivered power for a long time (the delivery time of a new large power transformer may be as long as 18 months) renders the great interest for methods that can be used to detect warning signals from a progressive deterioration.

A study about transformer failures carried out on transformers rated at 25 MVA or above for the period 1997 till 2001 was reported in [1]. The study shows that insulation failure is the leading cause of transformer failure. Table 1.1 lists the cost and number of failures for each cause of failure [1]. Another study [2] which categorizes failure rate with respect to transformer components reports that tap changer (41%), winding (19%), tank leakage (13%), bushing (12%), core (3%) and other (12%) are responsible for transformer failure.

Several methods can be used for monitoring of changes in the transformer. A nearly complete list of available methods for diagnostics of transformer is available in [3]. A few well known on-line methods that are used for transformer diagnostics are described in the following paragraphs.

Table 1.1. Cause of failures [1]

Cause of failure	Number	Total Paid [M USD]
Insulation Failure	24	150
Design/Material/Workmanship	22	65
Unknown	15	30
Oil contamination	4	12
Overloading	5	8.6
Fire/Explosion	3	8
Line Surge	4	5
Improper Maintenance/Operation	5	3.5
Flood	2	2.3
Loose connection	6	2.2
Lightning	3	0.66
Moisture	1	0.18
Total	94	287.44

### 1.1.1 Dissolved gas in oil analysis

The most common method used is dissolved gas analysis (DGA). DGA is the study of dissolved gas in a fluid such as transformer oil. Due to aging or electrical discharges the insulating materials inside the transformer breaks down and thus generate gases, which dissolve in the oil. The amount and distribution of these gases can be related to the type of fault. DGA gives signs about electrical sparks, partial discharge (PD) activity or thermal degradation due to elevated temperatures in parts of the transformer. Whenever the levels of hydrogen, hydrocarbon gases, moisture or other dissolved degradation by-products from the paper reaches a certain level, one needs to take some action to ensure the operating reliability and to prevent further deterioration or degradation.

### 1.1.2 Degree of Polymerization

Measurement of degree of polymerization (DP), which is correlated to tensile strength of paper insulation, can indicate the mechanical properties of paper insulation. Since it is not practical to take paper samples from an in-service transformer, an alternative method is used. Furanic components, which are one of the byproducts of paper ageing, become dissolved in oil and can be measured as an indication of DP or ageing prediction. The overall DP of the paper insulation in a

transformer can be inferred by measuring the types and quantity of furanic components in a transformer oil. This method can be used in order to confirm results from DGA. Lifetime estimation for a transformer according to DP is shown in [4].

### **1.1.3 Infrared thermography analysis**

By considering the fact that malfunction of most components in a system leads to increase in temperature, the idea of using thermography as a diagnostic tool has been developed. The increase of local temperature due to a fault results in a hot spot which may be detected by observing the heat pattern in a component of the system. Infrared thermography has been used to detect loose connections, unbalanced load and overload conditions, and potentially it can be used for diagnostics of other problems [3].

### **1.1.4 Mechanical diagnostic methods**

Switching a tap changer creates an acoustic signal which can be picked up by using piezoelectric sensors. The picked up signal would be different compared to a normal one if there is any change in the gears or switching contacts [3]. This is how mechanical diagnostic methods work. Stream analysis is another mechanical diagnostic method which is used to control the cooling system of a transformer. If there is any deformation in the winding it can affect the cooling system which can be detectable by stream analysis [5].

### **1.1.5 Electrical diagnostic methods**

A number of electrical diagnostic methods are available such as PD measurement, Dielectric Spectroscopy (DS), Polarization/depolarization current analysis (PDC), capacitance and power factor, winding resistance etc. PD measurement is one technique that can be used to identify the source of degradation. In a laboratory test on a transformer during manufacturing, identifying the type and cause of a defect in a transformer which has PD activity makes it easier and faster to fix the problem. A lot of work has been done on PD diagnostics but still there is a lack of comprehensive treatment of it. A common method for PD measurement is the Phase Resolved Partial Discharge Analysis (PRPDA) which shows the phase of PD occurrence and can possibly be used to determine the source of PD. This method also can provide other important parameters such as apparent charge and number of PD pulses. By performing PD measurement both in the time and phase domains one can extract

different parameters for PD activity, and it is possible to correlate these data to the source of PD.

The field seems to lack a comprehensive study about the dependency of PD characteristics on more realistic in-service conditions like increased temperature, paper- and oil humidity and different kinds of oil contamination; thus there is a need for more investigations in this area. Studying the change in the ageing state of an oil-impregnated system due to PD activity over time is also of great importance. Such change can show the state of the insulation system and it seems that investigation of this phenomenon could be very useful especially for the purpose of interpretation of on-line PD measurement results.

This study focused on developing a catalogue of signatures of PD defects that describe corresponding PD characteristics. The effect of temperature and humidity on PD parameters was investigated for some cases in papers I to IV. The effect of thermal ageing on PD activity as well as the effect of PD activity over time on oil-impregnated paper was investigated in paper V.

## **1.2 Literature review**

Different studies of Partial discharges have been conducted over the years and can be divided into works on detection and classification, localization and ageing. A brief summary of what has been done on PD classification and ageing over the last 20 years is provided here.

The purpose of PD classification is to determine the type of defect causing the PD (source of PD). One method for PD classification is to first develop simple models of defects and then analyze the PD characteristics corresponding to each defect. These models include void discharge, surface discharge in air and oil, corona discharge in air and oil, discharge in free bubbles in oil etc. Much of the work has been done on building a laboratory setup for generating different types of discharges. A summary of what has been done is given in the following paragraphs.

### **1.2.1 Corona in air**

Corona in air has been studied for a long time [6]. It is useful in some applications, for example ozone production and surface treatment. Corona can occur around the high voltage conductors of power transmission lines and will cause disturbing noise,

radio interference and increased power loss. It is normally not considered a dangerous discharge. However the behavior of corona is similar to other kinds of PDs and it can appear as a disturbance in on-line measurement.

### **1.2.2 Corona in oil**

Sustained corona discharge in oil can reduce its dielectric strength, and over time the corona activity could increase and finally result in oil breakdown and failure of the component [7]. The effect of parameters such as temperature, moisture and pressure on corona in oil is of importance especially for real application in power transformers. Increasing the temperature or the pressure of the oil results in reduction of the number of PD, while increasing the amount of moisture in oil results in increase of the number of PD [8]. The inception voltage and apparent charge for corona in oil are not dependent on oil age; however, the number of PD reduces as the oil age increases [8].

Negative corona in oil usually appears as a sequence of pulses. The effect of oil type and oil viscosity on the amount of charge and number of pulses in the PD pulse burst was investigated in [9-11]. The study shows that by increasing the applied voltage the number and the amplitude of PD pulses in the PD pulse burst increases [9-11]. Based on apparent charges which were transformed for producing first discrete PD pulse they estimated that the size of micro cavity could be in the order of 2 micrometer. A thorough investigation of the phenomena before breakdown in oil is given in [12]. This study shows that with negative polarity, generation of micro cavities (10 micrometer in diameter) precedes the development of streamers. It also concluded that the inception voltage for negative corona is slightly less than for positive corona. An investigation of positive and negative corona in oil was carried out in [13]. The result focused on pulse shape, amount of charge, and inception voltage for positive and negative corona in oil as a function of the needle tip radius.

### **1.2.3 Surface discharge in oil**

Pressboard is frequently used inside power transformers as insulation. Between the high voltage and low voltage winding there is a gap which is subdivided into many oil ducts by means of solid insulating barriers. This combination of oil and pressboard gives a higher dielectric strength than individually. However due to complications in the transformer design there are places where the field component is parallel to the insulation surface. This reduces the strength significantly, and surface

discharges may occur. Surface discharge in oil has been investigated in [14-21]. Results from a needle-bar electrode configuration used for generating surface discharge in oil indicate that there is a difference between surface tracking and surface flash-over. The results show that the tracking is the result of surface discharge, and that the surface discharge and surface flash-over are two distinct phenomena [14-16]. Experiments on surface discharge in an oil-pressboard interface with different ageing degree indicate that PD repetition rate and maximum PD magnitude would increase by increasing the applied voltage. The oil ageing has a lot of influence while the pressboard ageing has little effect on PD characteristic over oil-pressboard interface [17]. Investigation of the influence of the electrode geometry on surface discharge in oil shows that different electric field distributions cause different damage on the pressboard [18]. Investigation of the surface discharge in the oil-pressboard interface by using a needle-plate electrode configuration shows that a trace of carbon which is the result of surface flashover could moderate electric field around the needle and thus reduce the PD activity [19]. Studies of the effect of temperature on surface discharge in oil-pressboard interface shows that the increase in temperature could cause faster development of PD. Studies also show that at high temperature the inception voltage is much lower than at low temperature [20, 21].

#### **1.2.4 Bubble in oil**

Nitrogen from the expansion space in an oil-impregnated bushing can be dissolved into oil if the temperature of bushing is increased. If rapid cooling takes place, bubbles may appear due to oversaturation of the oil. Bubble evolution in bushings was investigated in [22]. Bubbles could also be generated in an overloaded transformer. The hotspot temperature on the winding determines the bubble evolution. The limits of overloading with respect to the winding hot spot were investigated in [23]. Investigation of bubble behavior under AC electric field was performed in [24]. The authors of [24] classified the behavior of bubbles in oil broadly into turbulence type (large bubbles) and non-turbulence type (small and medium bubbles). They concluded that turbulence bubbles are harmful because the volume of bubble keeps increasing once PD starts. Comparison between the PD pattern due to moving bubbles in a region with high electric field and the PD pattern due to bubbles between layers of paper was performed in [25]. They characterized PD due to bubbles in oil by symmetric patterns which cover almost entirely the phase range. Their results show that PD magnitude may vary a lot and the repetition rate depends



on the average size of bubbles, very low for small bubbles and higher for larger bubbles.

### **1.2.5 Cavity between layers of paper**

Cavities inside the insulation may appear due to bad manufacturing or due to ageing of the insulation material. Usually the electric field inside a cavity is higher than the electric field on the surrounding insulation material. PD activity in a cavity over time degrades the insulation by means of chemical byproducts and particle bombardment which finally could lead to complete breakdown. Due to the simplicity of this defect it is possible to predict a general PD pattern corresponding to this defect, which is explained in Chapter 2. The effect of the number of voids and their relative position inside the insulation on PD pattern is presented in [26], and experimental results for PD activity in a cavity and its modeling are shown in [27].

### **1.2.6 PD Classification**

Classification of PD with the aim of recognition of the unknown origin has been performed for many years by using an experienced operator to study discharge patterns on the well-known ellipse on an oscilloscope screen [28]. Since the early 1990s many papers [29-33] have been published with the main idea of using computer in order to classify the PD patterns. The main approach of all of these papers is to first build a data bank of PD patterns. This data bank has been made by using small scale laboratory setups which simulate the defects that can produce PD. In the second stage after recording all PD patterns corresponding to different defects, different features of the PD patterns are extracted. In the third stage comparison between these features lead to classification of the PD patterns. The main PD patterns which are currently used for classification are phase-resolved PD data, time-resolved data and data without phase/time information. In order to classify the features a number of methods have been proposed during the last 20 years. For example, one can mention methods like distance function, statistical, artificial neural network based and fuzzy logic based classifiers. Each of these methods employs a different strategy for classification which is briefly explained in [34].

### **1.2.7 PD ageing**

PD causes deterioration due to mainly two mechanisms: chemical reactions between the ionized gas (such as nitric acids and ozone) and the oil-impregnated paper, and direct physical attack by ion and electron bombardment causing bond-scissions [35-37]. A review on degradation of solid dielectrics due to internal discharge is given in [37]. Investigation of the ageing of epoxy-paper insulation in transformers through partial discharge analysis shows that the PD inception voltage drops significantly at the initial stage of the ageing test but after that it becomes relatively stable for the remainder of the ageing test [38]. Studies of the effect of ageing on PD activity in the pressboard-oil interface showed that the pressboard ageing has little influence but instead oil ageing has great influence on PD characteristics over an oil-pressboard interface [39]. The harmful PD level which decreases the residual lightning impulse withstands voltage on oil impregnated pressboard insulation has been investigated in [40]. The study shows that PD magnitudes less than 10000 pC barely reduce lightning impulse withstand voltage compared to new pressboard, but for PD magnitudes above 20000 pC the lightning impulse withstand voltage tends to decrease compared with that of new pressboard.

### **1.3 Aim**

The aim of this thesis is to achieve a deeper insight into the signatures and degradation rates of defects that generate partial discharges in power transformers. The objectives are to design physically realistic experimental objects, perform experiments on these and create models that can explain their behavior. The defined experiments are studied under different physical conditions in order to find the dependence on temperature, humidity, oil contamination and different situations of ageing. For example with respect to paper ageing: different levels of moisture, degrees of depolymerization and thermal aging. The progress of the PD activity over time and under different ageing conditions is investigated.

### **1.4 Thesis outline**

This licentiate thesis consists of six papers which are appended at the end of this thesis. A summary of those papers is given in Chapter 8. A background to this work and an overview of previous work are given in Chapter 1. Basics of partial discharges, equivalent circuit and detections methods are discussed in Chapter 2. In Chapter 3

experimental setups and measurement systems are introduced. Classification of partial discharge by using appropriate parameters which are driven from both time domain and phase domain is given in Chapter 4. All tested defects that may generate PD inside transformer are summarized in Chapter 4; however the full discussion for each defect is presented in the attached papers. A discussion of the PD activities which may occur outside a transformer and appear in the PD measurement is given in Chapter 5. The effect of temperature on partial discharge behavior in oil is discussed in Chapter 6. Deterioration of oil-impregnated paper due to PD activity over time is discussed in Chapter 7. Chapter 8 gives a summary about the papers I - IV. General conclusions and future work are presented in Chapter 9.

### **1.5 Author's contributions**

The author is responsible for Papers I-IV and Paper VI. In Paper I-IV by use of experimental test setups general characteristics of PD due to different possible defects in a power transformer were extracted. In Paper I the effect of humidity on corona in oil was investigated. In Papers I and III and IV the effect of temperature on PD inception voltage was investigated.

Papers V and VI are joint papers where the author worked together with Respicius Clemence Kiiza. In Paper V, which is part one of the joint papers, the author participated in measurement and in discussion for interpreting results. The effect of high voltage impulses on PD activity on oil-impregnated paper was investigated in paper V. In Paper VI, which author is fully responsible for, the ageing of oil-impregnated paper due to PD activity and the effect of thermal ageing on PD activity is discussed.

This work has been supervised by Assoc. Prof. Hans Edin (KTH Electrical Engineering)



## Chapter 2

### PD Basics, Equivalent Circuit and Detection

A partial discharge (PD) is a localized electrical discharge in an insulation system which is limited to a small part of the dielectric and only partially bridges the insulation between the electrodes.

PD usually occurs due to the existence of either a highly non uniform electric field, as in corona discharge, or in a situation where the insulation has a weak point, like in a gas-filled defect. PD has the deteriorating effect and over time it reduces the lifetime of an insulation system. During PD phenomena on the surface or inside an electrical insulation, high energy electrons or ions cause deterioration of the insulation material. This bombardment may result in chemical decomposition in the insulation material, which could finally lead to complete breakdown of the insulation.

#### 2.1 Types of partial discharges

Partial discharges can be divided into five main groups including internal, surface, corona, electrical treeing and barrier discharges.

##### 2.1.1 Internal discharge

Internal discharges are normally due to cavities inside an electrical insulation. Cavities inside the insulation could be because of bad manufacturing or they can be created due to ageing of insulation material.

The electric field inside a cavity is equal to or greater than (depending on the geometry of the cavity) the electric field in the surrounding insulation. Also air has lower electric breakdown strength than the surrounding insulation and as a result cavities are weak points inside the insulation. The breakdown electric field for dry air at 20 °C and 1 bar is 4.7 kV for a 1 mm air gap between electrodes. If the electric field inside the cavity is high enough, PD activity is initiated. Figure 2.1 shows different kinds of cavity in a solid insulation.

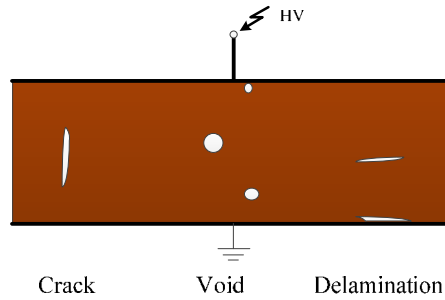


Figure 2.1: Different kinds of cavities in a solid insulation

### 2.1.2 Surface discharge

Surface discharge is a kind of PD that occurs along the surface of solid insulation in contact with gas or liquid insulation. The discharge can be initiated in the region with high electric field, but can then propagate into the area that has not enough stress to initiate surface discharge. Surface discharge occurs since the dielectric strength on the interface of dielectric insulations is less than dielectric strength of each one. Surface discharge may occur in the end of cables if there is a bad grading for the cable termination. It can also occur in bushings or on line-insulator surfaces. Figure 2.2 shows places where surface discharge may occur. During the design process of high voltage equipment, placing the interface of dielectric insulations in the direction of the equipotential lines can reduce the probability of surface discharges occurring. In situations where it is not practical to place the interface in the direction of the equipotential lines it is better to place the interface at a large angle with the electric field lines.

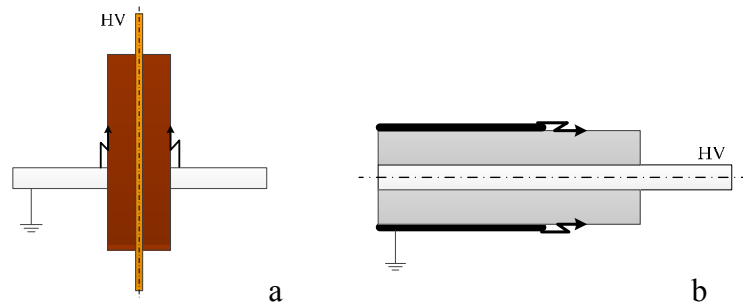


Figure 2.2: Surface discharge, a) on the bushing surface close to the transformer flange, b) on the end of outer semiconductor in a cable termination

### 2.1.3 Corona

Corona is a kind of discharge that occurs around sharp conducting points or bare conductors at high voltage (highly divergent field) either in air, other gases or in a liquid such as transformer oil. Corona may also occur at a sharp point at ground potential.

### 2.1.4 Electrical treeing

Existence of high electric field inside a dielectric material can cause initiation and propagation of an electrical tree. Electrical treeing could originate from a defective point as a small gas void, sharp electrode-edge or metallic particle, where the electric field is high. This high electric field can cause partial discharge in a gas filled void in the dielectric, and generate ozone and ultraviolet light as a byproduct that further can react with the dielectric material and cause decomposition of the dielectric and generation of a new void. This weak point grows up over time and makes a branched electrical tree inside the bulk of the insulation. This tree can grow up to the point that it causes complete breakdown. In the same way, 2D electrical treeing can happen on the surface of a dielectric that has been subjected to high electric field or it can happen due to a contamination such as salt on the surface of the insulator and cause flashover across the surface.

### 2.1.5 Dielectric barrier discharge (DBD)

This kind of discharge is usually generated intentionally and it is widely used in the treatment of fabrics. DBDs are characterized by insulation layers (generally glass or silica glass or ceramic materials) on one or both electrodes or on dielectric structures inside the discharge gap [41]. Figure 2.3 shows examples of corona discharges, electrical treeing and DBD.

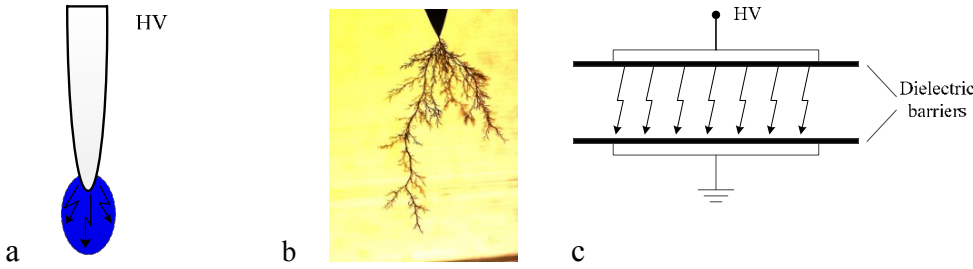


Figure 2.3: a) Corona discharge, b) Electrical treeing inside solid insulation, c) DBD

### 2.2 PD equivalent circuit

Consider a cavity inside a solid insulation as shown in figure 2.4. The cavity can be modeled with capacitor  $C_c$  in parallel with an air gap which acts as a controlled switch with voltage across the cavity. Capacitors  $C'_b$  and  $C''_b$  show the capacitance of the part of insulation in series with the cavity and capacitors  $C'_a$  and  $C''_a$  show the capacitance of the bulk of insulation parallel to the cavity. Figure 2.5 shows the simplification of figure 2.4.

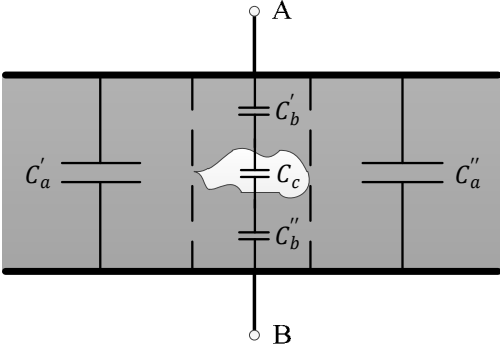


Figure 2.4: Cavity inside an insulation material and equivalent capacitances for different parts of the insulation

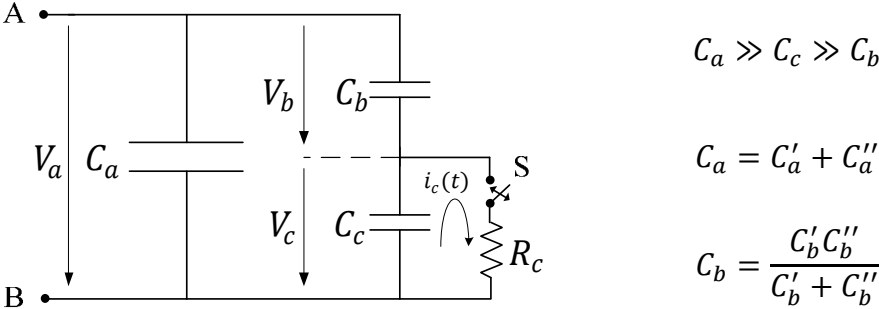


Figure 2.5: Equivalent circuit for PD

By increasing the voltage between terminals A and B, the electric field inside the cavity increases and finally PD occurs. In figure 2.5 when the switch S is closed, a discharge current  $i_c$  flows for a very short time. The resistor  $R_c$  ensures that the



magnitude of the current is limited. If an AC voltage  $V_a$  is applied to terminals A and B, there is a potential drop  $V_c$  across the cavity. By increasing the terminal voltage all capacitors charge up. As the capacitor  $C_c$  is charging, the voltage across it increases. The voltage across the cavity that is equal to the voltage across capacitor  $C_c$  increases until it reaches a certain voltage (which is dependent on the geometry, type and pressure of the gas inside the cavity) where electric breakdown occurs inside the cavity and the capacitor  $C_c$  is discharged down to the voltage that is needed for quenching the discharge pulse. When the discharge current is extinguished, again the capacitor  $C_c$  starts to charge up and the same process repeats for the next occurring partial discharge. Charging and discharging of the capacitor  $C_c$  results in PD current pulses.

Figure 2.6 shows how PD pulses are generated in relation to the applied voltage. In this figure  $V_c$  is the voltage across the cavity which is a fraction of applied voltage ( $V_a$ ). When the voltage across the cavity reaches  $U^+$ , which is the breakdown voltage of the gas inside the cavity, a discharge occurs and the voltage across the cavity drops to  $V^+$  where the discharge extinguishes. Corresponding to the applied voltage which is increasing, the voltage across the cavity increases again and another discharge occurs. By decreasing the applied voltage the voltage across the cavity increases in the reverse polarity and when it reaches  $U^-$  a PD pulse occurs with negative polarity and the voltage across the cavity drops to  $V^-$  and the process is repeated in the following cycles [35, 42].

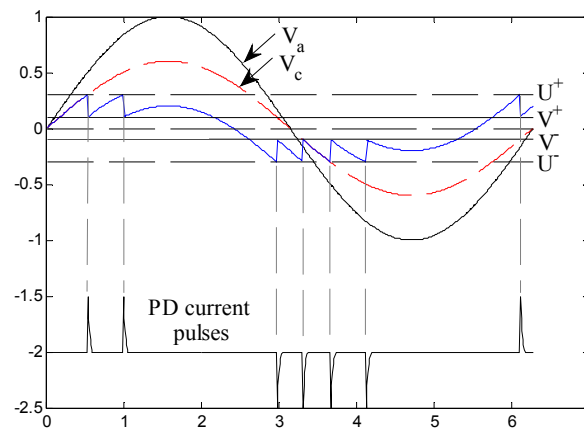


Figure 2.6: Repetition of partial discharge pulses in a cavity exposed to high alternating voltage

The same kind of modeling (abc model) can be used in order to make simple and conceptual models of surface discharges and corona discharges and is fully explained in [35]. However, prediction of the PD pattern is not as easy as for internal discharges. Using the concept of space charge and space charge build-up near a sharp point it is possible to explain why negative corona starts sooner than positive corona [42]. However changes of corona pattern at different voltage level remain to be explained. The change of corona pattern due to different voltage levels is shown in Chapter 5. Experimental results for surface discharge in air shows that the PD pattern is strongly dependent on the geometry of the electrodes. This result is presented in Chapter 5.

### **2.3 PD detection and localization**

Partial discharge is accompanied by several phenomena such as light and electromagnetic radiation, sound generation, dielectric losses, chemical reaction, increased gas pressure and electrical current pulses. By sensing any of the above phenomena one can detect partial discharges. For transformer PD monitoring mainly electrical, acoustic and chemical detection has been used.

#### **2.3.1 Electrical detection**

The electrical PD measurement system consists of coupling sensors and data acquisition units. Two types of sensors are usually used for PD measurement in transformers: capacitive and inductive coupling sensors. The bushing tap available in transformers allows using the grading foil layer inside the bushing as a capacitive coupling sensor. If the bushing tap is connected to ground using a wire, it is possible to measure the current passing through that wire by means of a High Frequency Current Transformer (HFCT) which is an inductive coupling sensor. During online measurements, in order to distinguish external disturbances coming from the transmission line connected to the bushing from the PD signals inside the transformer, a Rogowski Coil wrapped around the bushing together with the bushing tap can be used. A list of commercially available acquisition units for online monitoring of transformers is given in [28]. The main advantages of the electrical measurement are its accuracy, information about PD intensity, and possible determination of the defect type and PD source. However the electrical interface is a drawback during on-line measurements. During off-line measurements, and especially the PD test performed

by transformer manufacturers in a shielded laboratory, the electrical method is usually used due to its high accuracy.

A circuit for PD detection is shown in figure 2.7. This circuit contains of the power supply, coupling capacitor, test object, and detection impedance. The detection impedance could be in series with the test object or with the coupling capacitor. If it is in series with the test object it is more sensitive in measuring PD pulses since all the PD pulses have to pass through the detection impedance. However this connection has the problem that if a complete breakdown occurs in the test object, it could damage the measurement system. On the other hand if the detection impedance is in series with the coupling capacitor the above problem is eliminated which is why this is the common method. However in such an arrangement the measured signal could be noisier. A typical PD measurement system connection on a power transformer is shown in figure 2.8.

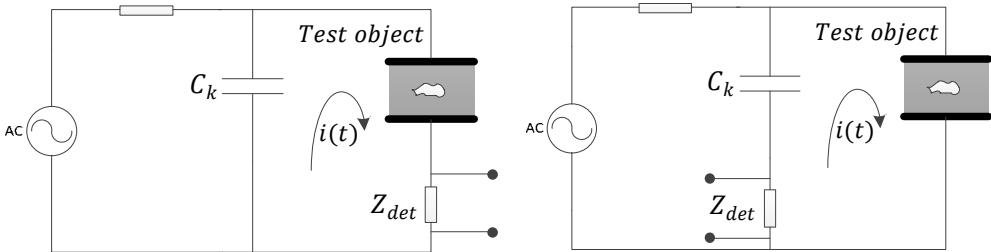


Figure 2.7: Measurement of apparent charge, different location for detection impedance

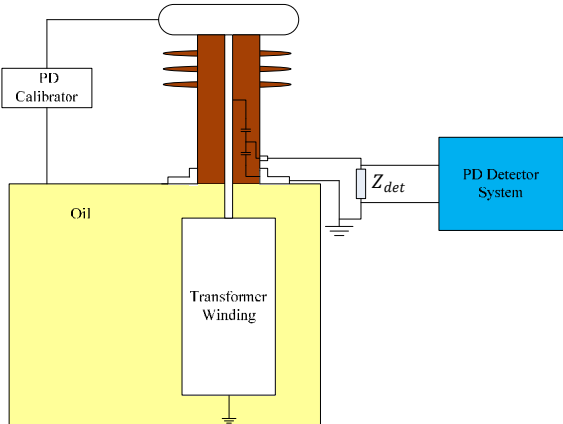


Figure 2.8: PD calibration and measurement connection for transformers with capacitive tap on the bushing

### **2.3.2 Acoustic detection**

PD is accompanied by sound generation. The acoustic wave, audible or not, is due to the expansion of gases near the discharge channel, which propagates as a pressure wave. This acoustic signal can be detected by piezoelectric transducers, condenser microphones, accelerometers, fiber optic acoustic sensors and sound-resistance sensors. The main frequency used for acoustic detection is between 10 kHz to 1000 kHz [28] and usually ultra-sonic PD detectors are tuned at 40 kHz.

An advantage of acoustic detection is the ability to use multiple sensors in different positions on the transformer tank in order to localize the PD source, as well as being immune against electrical interference. Immunity against electrical interference does not mean that there is no acoustic noise in the environment. Mechanical noise from the transformer core is the main source of acoustic noise; however the frequency content of these vibrations is sufficiently lower than the PD acoustic signal [43]. According to comments from a specialist from Physical Acoustic Inc. this method doesn't work well in open air during a rainy day.

This method has low sensitivity and in particular it cannot detect void discharges unless they are very big. Also the acoustic propagation pathway can be very complex, which is the main disadvantage of the acoustic PD detection. Another issue is the cost of commercially available acoustic sensors and their amplifier which is relatively expensive. A master thesis has been published at KTH, investigating the possibility of designing cheap sensors and amplifiers for acoustic PD detection [43].

### **2.3.3 Chemical detection**

Detection of chemical byproducts produced by PD activity is one of the simplest methods for PD detection. This method is widely used in transformers by means of Dissolved Gas Analysis (DGA) with Duval Triangle diagnostics. The method is also applicable in Gas Insulated Substation (GIS) where analysis and detection of SF<sub>6</sub> gas components can be used. The main advantage of this method is that it is very well established, immune against noises and relatively easy to measure. However it cannot say much about the type of defect, location and intensity of PD, which is the main disadvantage for this method.

#### **2.3.4 PD localization**

The aim of PD localization is to locate the PD source in an apparatus. PD localization is of importance in power transformers since they are bulky and it is not practical to open a transformer and search for a PD source inside it. The most common method for localizing a PD source in a transformer is using acoustic PD detection. In this method many sensors (at least three) are placed on the transformer wall. When a PD occurs the generated sound travels to all sensors. Considering the arrival time to each sensor and the speed of sound propagation in the oil, paper and metallic tank, it is possible to find the distance from the PD to each sensor and therefore to locate the PD inside transformer [44]. While the acoustic PD localization is a well-known method, many researchers have investigated the possibility of electrical localization [45]. In these methods usually PD signals are recorded both from the bushing and neutral of the transformer, and by using some transfer function it is possible to predict where is the PD source along the winding [46, 47]. Even though the results obtained by these methods are somewhat satisfactory, it has been shown not to be very reliable, especially when the PD occurs in the middle of the winding [46].



## Chapter 3

### Measurement systems

#### 3.1 PD measurement System

Most of the measurements were performed by using a common PD measurement method which is Phase Resolved Partial Discharge Analysis. In this method PDs are recorded with respect to the phase of the applied voltage. The entire PD patterns were recorded by using a commercial instrument which is designed according to IEC-60270. This is the ICM-system (Insulation Condition Monitor) from Power Diagnostix Systems GmbH [48]. A schematic of the basic parts and connection to ICM system is shown in figure 3.1. Because of PD occurrence the apparent charge  $q_{app}$  transferred from the coupling capacitor to the test object. This apparent charge passes through the detection impedance and builds a voltage across it, which is amplified by a preamplifier which normally should be placed near the signal source. The amplified PD pulse enters the main amplifier mounted on the ICM-system. Through the main amplifier the PD pulse is further amplified and sent to an analogue to digital converter. PD pulses that are higher than a low-level discriminator level (LLD) (a threshold level for detection level set in order to reduce noise) are detected in the analog-to-digital converter (ADC) and sorted into phase and charge channels. Phase has 256 levels for the interval 0-360° and charge has 128 positive and 128 negative levels.

The output from the measurement system (sent to a computer) is a 256×256 matrix where each column represents a phase level, each row a charge level, and each element the number of PD pulses with the specific phase and charge level.

Prior to each measurement one has to calibrate the system in order to make different measurements comparable. The calibrator that is used in this work is CAL1D from the Power Diagnostix Systems. It can inject a known charge between 10 pC to 1 nC. The calibrator must be connected across the test object when the voltage is off and by using the ICM software one can calibrate the measurement system. A photo of the ICM system and the PD calibrator is shown in figure 3.2. A more detailed description of the ICM system can be found in [41, 49].

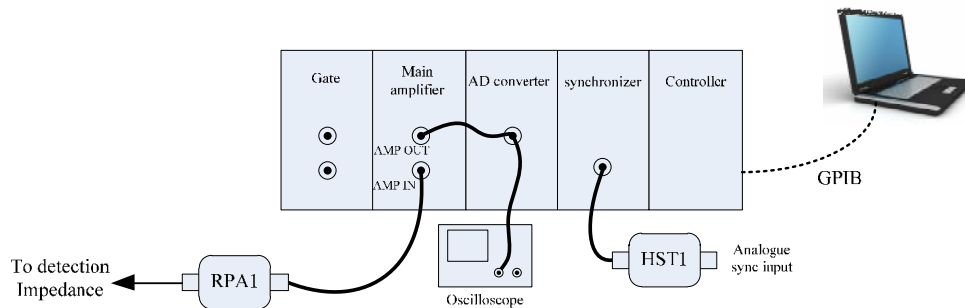


Figure 3.1: Schematic of the basic parts and connections of the ICM system

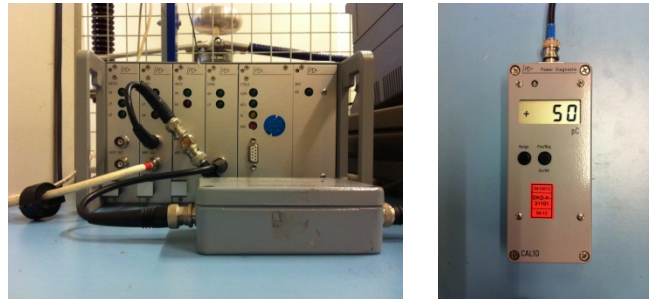


Figure 3.2: ICM system with synchronizer (left hand side) and PD calibrator (right hand side)

Two equipments for voltage supply were used during the experiments. In most experiments a high voltage step up transformer with maximum output of 100 kV was used. The output voltage was controlled by a variable transformer in the control unit. The other one is an amplifier whose details are given on the next page.

In order to record individual PD waveforms with high resolution, a high bandwidth detection system based was designed. A 50 ohm resistance was used in series with the test object. A voltage drop on this detection impedance can be measured by a fast oscilloscope in order to obtain a PD signal in the time domain with high resolution. In this thesis an oscilloscope (Tektronix TDS 3052) with 500 MHz bandwidth and 5 GSample/s was used. A schematic of the measurement system when the high voltage transformer was used as a voltage source is shown in figure 3.3.



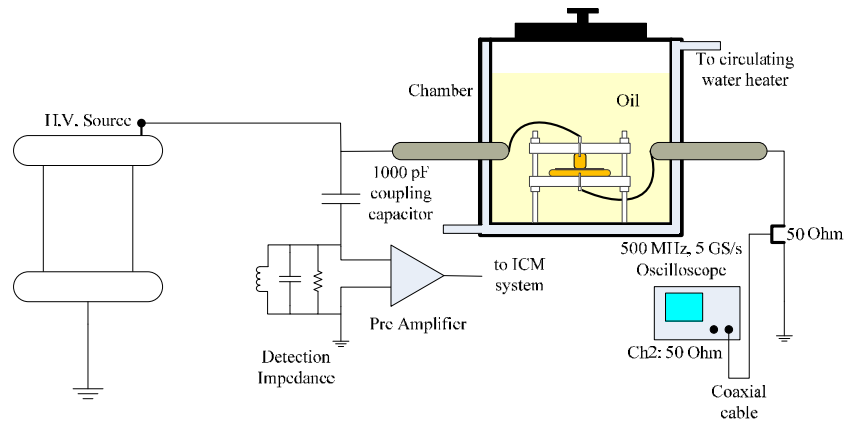


Figure 3.3: A schematic of PD measurement system with a high voltage transformer as the power supply

In the ageing experiments due to a limitation of the high voltage transformer (the voltage can only be controlled manually and it cannot trip in the case of breakdown) a voltage amplifier was used. The schematic of the measurement system which was used to study ageing by PD activity is shown in figure 3.4. The measurement system consists of a TREK 30/30 high voltage amplifier which has maximum output of 30 kV. The amplifier input is fed from a function generator (HP 3245A) controlled by a computer through GPIB. In order to eliminate switching noises from the high voltage amplifier a low pass filter was used. The capacitor in the low pass filter also acts as a coupling capacitor for these measurements. Pre-amplified PD signals are also connected to a Tektronix Oscilloscope for acquisition in the time domain. By using a calibrator it was shown that the measurement sensitivity was 5 pC. This somewhat low sensitivity is due to noise from the power supply; however the sensitivity is very satisfactory compared to magnitude of discharges occurring in the samples.

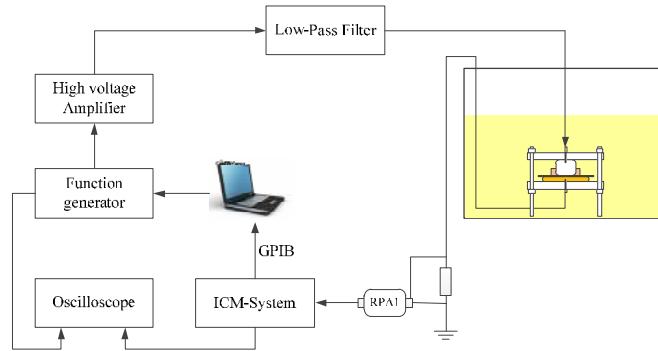


Figure 3.4: A schematic of the PD measurement system with high voltage amplifier as a power supply

### 3.2 Dielectric spectroscopy measurement in frequency domain

In order to check the ageing state of the oil-impregnated paper after exposure to PD, measurements of dielectric spectroscopy and polarization and depolarization current were performed.

The complex permittivity was measured using the IDA200 dielectric spectroscopy analyzer. This means that the output of IDA200 is  $C'$  and  $C''$ . IDA200 is shown in figure 3.5.



Figure 3.5: The IDA200 dielectric spectroscopy analyzer

A drawing of the test cell used is shown in figure 3.6. The electrodes of this test cell are made of stainless steel. The ground electrode (Lo) is separated by a 1 mm air gap from the guard electrode. The thickness of the ground electrode is 2 mm in order to minimize possible leakage currents between the ground and guard electrode. The Lo electrode is loaded by a spring which makes the pressure equal for all measurements.

All electrical connections from IDA200 to the test cell were made according to figure 3.7.

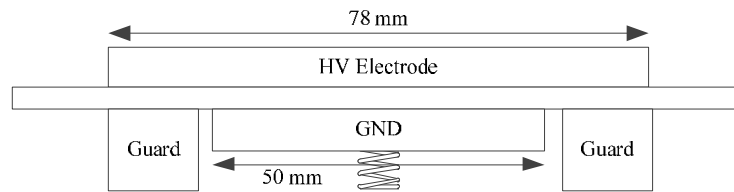


Figure 3.6: Test cell for measuring dielectric spectroscopy

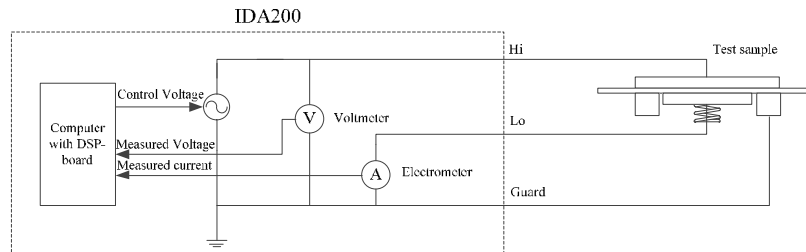


Figure 3.7: Measurement circuit for measuring dielectric spectroscopy

### 3.3 Polarization and depolarization current measurement

The polarization and depolarization current was measured by a KEITHLEY 614 electrometer and a DC power source which can generate a voltage up to 3 kV. The sample was placed between two metallic electrodes (similar to that in figure 6 with an additional metallic box which covers the test cell totally to protect against any disturbances) and the polarization current was measured with the electrometer. A photo of the polarization current measurement system is show in figure 3.8.



Figure 3.8: Polarization current measurement system



## Chapter 4

### Partial discharge classification

#### 4.1 Formats of data saving

The response of a low or narrow bandwidth measurement system is completely different from the real PD waveform and the only useful parameter from this kind of measurement is the apparent charge. However due to the short response time compared to the 50 Hz cycle it is possible to distinguish the phase of PD occurrence with this kind of measurement systems. This kind of data is phase domain data which can be recorded by two methods, Phase Resolved Partial Discharge Analysis (PRPDA) and Pulse Sequence Analysis (PSA).

On the other hand, very high bandwidth measurement systems can measure the PD waveform in the time domain. This kind of data is called time domain data and can be obtained through Time Resolved Partial Discharge Analysis (TRPDA).

##### 4.1.1 Phase Resolved Partial Discharge Analysis (PRPDA)

In this method, the phase of occurrence, apparent charge and number of PDs which has the same phase and magnitude can be recorded. For data recording purpose usually a  $m \times n$  matrix is used where  $m$  is the number of phase channels and  $n$  is the number of charge levels. Each element of this matrix shows the number of PDs with a particular magnitude and phase. This method can provide different patterns such as  $\varphi - n$  pattern (the phase of occurrence versus the number of PD),  $\varphi - q_m$  pattern (the phase of occurrence versus the maximum apparent charge),  $\varphi - q_a$  pattern (the phase of occurrence versus the average apparent charge),  $q - n$  pattern (the apparent charge versus the number of discharge) and  $\varphi - q - n$  pattern which is a 3D pattern and shows the number of PD, phase of occurrence and magnitude of PD. Figure 4.1 shows different kind of patterns for PD related to a cavity discharge.

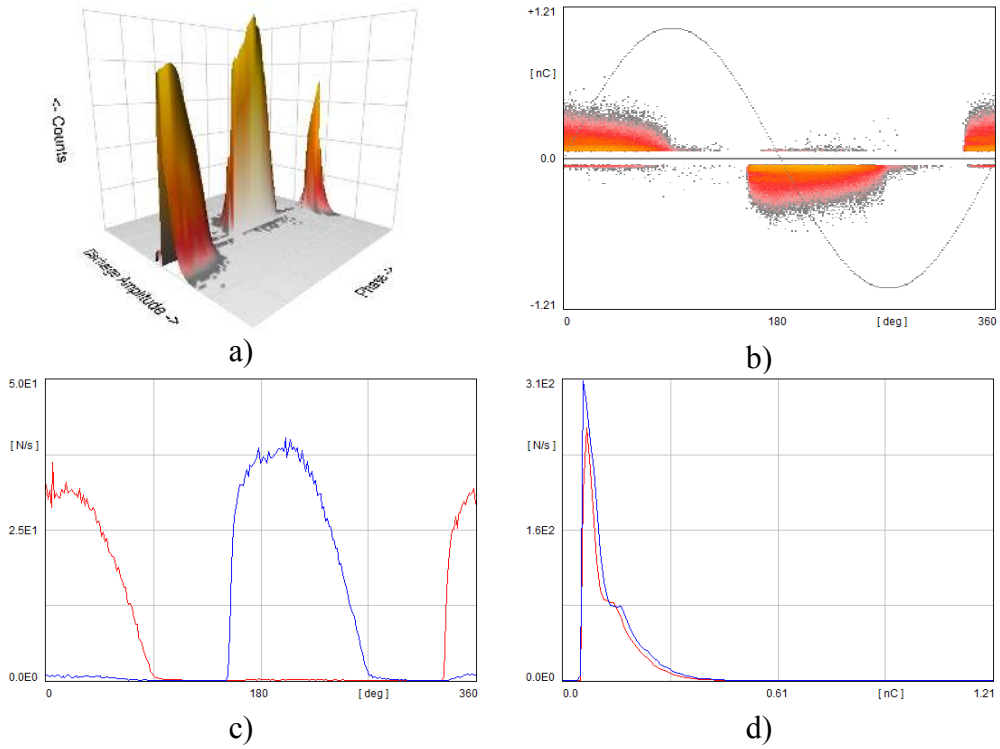


Figure 4.1: Different PD patterns obtained from PRPDA, a)  $\varphi - q - n$  pattern, b)  $\varphi - q$  pattern, c)  $\varphi - n$  pattern, d)  $q - n$  pattern

#### 4.1.2 Pulse Sequence Analysis (PSA)

PD pulses deposit ions and electrons at the place of occurrence. Due to the very low surface and bulk conductivity of the insulation system, those kinds of particles remain in place for a longer time compared to the average time between two consecutive PD pulses. This means that the physical condition for next pulse will be affected by the previous PD pulse. Since in PRPDA all data is recorded as a cumulative matrix and sequences of PDs are not considered, this method cannot provide anything about the effect of previous PD pulses. In order to solve this problem, PSA was proposed where data related to PD pulses should be saved as a sequence of data. In this method for each PD pulse an element of  $(q_i, u_i, t_i)$  is added to the recorded data where  $q_i$  is the apparent charge,  $u_i$  is the voltage and  $t_i$  is the time when the PD pulse occurred. PSA clearly has more interesting parameters (such as the voltage at the instance of a discharge) compared to PRPDA.

Not only are all those patterns mentioned for PRPDA implementable by PSA, but also two more patterns can be generated using this method. In the first pattern each PD pulse will be represented by a point in the  $t - \varphi$  plane where the color of the point indicates the magnitude of the PD. This pattern is useful for investigating the change of PD activity over time. The second one is  $\Delta u_i - \Delta u_{i-1}$  pattern. In this pattern each PD pulse is represented by a point in a 2D graph. In this graph the x-axis represents the voltage difference at the instant of one PD pulse compared to the previous PD pulse and the y-axis represents the voltage difference at the instant of one PD pulse compared to next PD pulse.

#### 4.1.3 Time Resolved Partial Discharge Analysis (TRPDA)

To make PD classification possible one has to choose suitable characteristics in order to make separation between different types of PDs easy and possible. Interesting parameters in TRPDA could be the peak value, rise time (time span in which the PD signal reaches from 10% to 90% of its peak), fall time (time span in which the PD signal reaches from 90% to 10% of its peak at the tail of signal), pulse width (time span between 50% of the peak on the front and tail of the pulse), pulse duration (time span between 10% of the peak on the front and tail of the pulse) and apparent charge (can be obtained by taking an integral of the PD pulse). A typical PD waveform in the time domain is shown in figure 4.2.

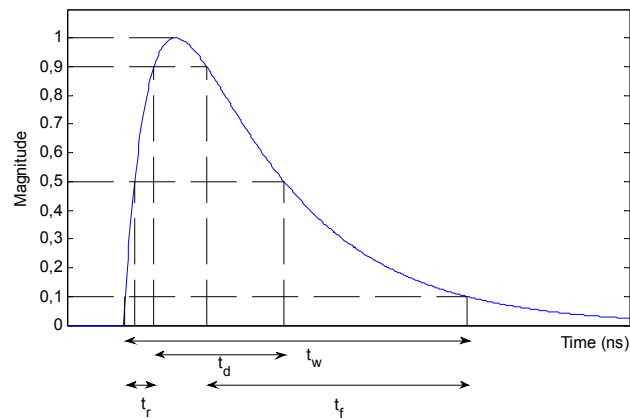


Figure 4.2: A typical PD waveform in Time domain

The TRPDA has all the data (such as apparent charge, phase of occurrence, voltage level at the instance of occurrence and pulse sequences) obtained from PSA, plus further interesting parameters (such as rise time, fall time, pulse duration and pulse

width) which can be used for classification. However, at least two issues limit the usage of this method. First, the PD waveform measured at the transformer bushing can be affected by its position along the transformer winding. This means that all the advantages of this method compared to PSA can be undermined. The second issue is the huge volume of the data recorded in time domain. Considering 20 ms (one 50 Hz cycle) measurement time with 100 MSample/s sampling rate, the recorded file would be around 8 MByte. Recording the signal for 1 minute it would require 24 Gbyte. Saving and processing these amounts of data produce difficulties. However, by using a suitable computer program it is possible to take the interesting parameters in time domain immediately after capturing the signals and only record those parameters and not the whole PD waveform.

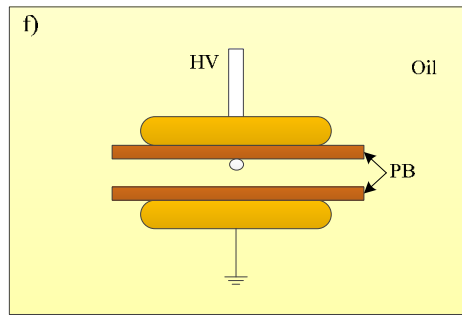
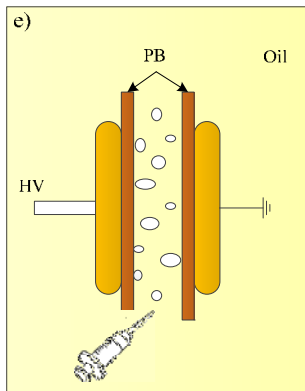
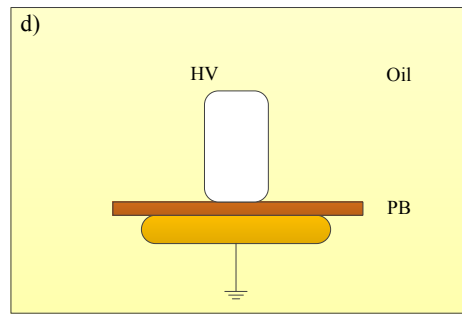
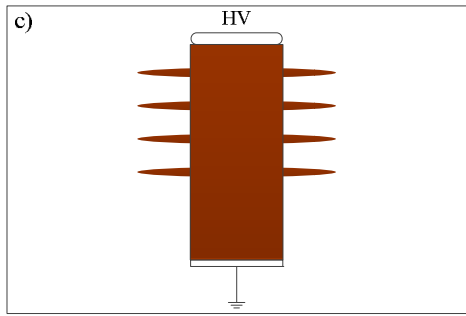
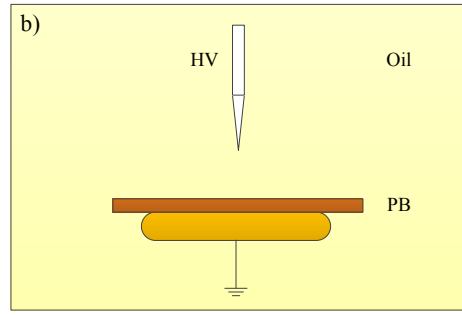
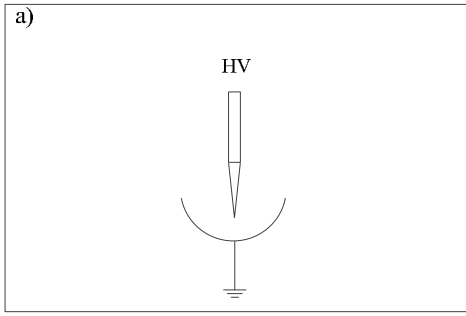
#### **4.2 PDs on the insulating system consisting of oil and oil-impregnated paper**

Discussion about PDs on the insulating system consisting of oil and oil-impregnated paper was performed in the attached papers. Corona in oil was investigated in paper I, bubble in oil in paper II and III, metal object at floating potential in paper III, void discharge in paper VI, and surface discharge in oil in paper IV.

#### **4.3 Phase domain and Time domain characteristics**

A schematic of the tested defects is shown in figure 4.3. All the PD sources and their corresponding PD patterns and waveforms that were tested during this licentiate thesis are summarized in table 4.1 and table 4.2 respectively. In front of each PD pattern and waveform the general characteristics related to that pattern and waveform is mentioned. These characteristics could be useful for the purpose of classification.





Continued on next page

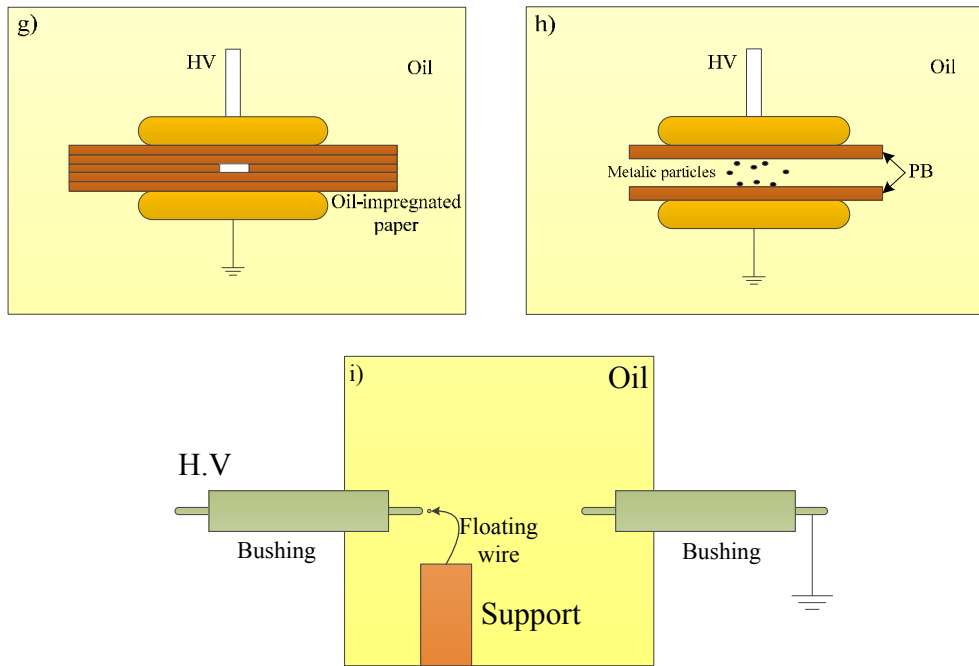
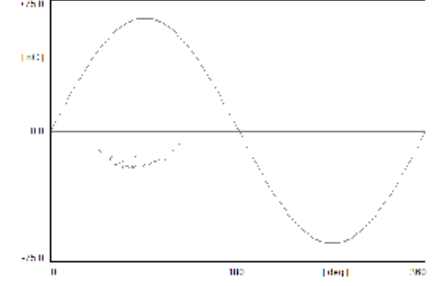
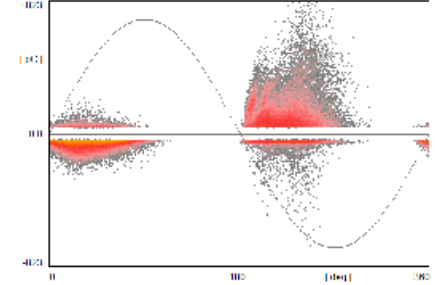
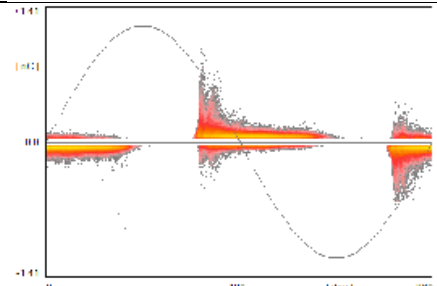
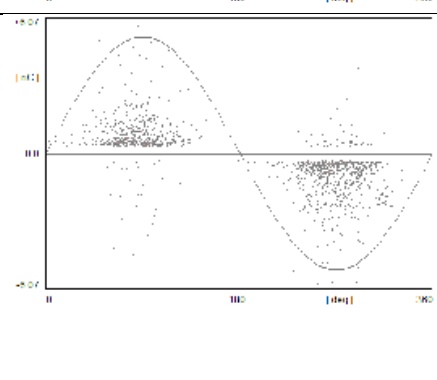


Figure 4.3: Schematic of possible defects which may generate partial discharge inside a transformer, a) corona in air, b) corona in oil, c) surface discharge in air, d) surface discharge in oil, e) free moving bubble in oil, f) bubble adjacent to pressboard, g) cavity between layers of paper, h) free metallic particle in oil, i) metallic object at floating potential

Table 4.1: Results corresponding to figure 4.2

	Characteristic PD pattern	Characteristics
Negative corona in air (4.2-a)		<ul style="list-style-type: none"> <li>• Phase of occurrence: around 270°</li> <li>• Magnitude: small</li> <li>• The magnitude of discharge depends on the radius of the sharp point and it is fairly constant with voltage change</li> <li>• Repetition rate strongly depends on voltage level</li> <li>• Repetition rate (at 10% above the inception voltage): very high</li> <li>• Inception voltage is lower than positive corona in air</li> </ul>
Positive corona in air (4.2-a)		<ul style="list-style-type: none"> <li>• Phase of occurrence: around 90°</li> <li>• Magnitude: large</li> <li>• The magnitude of discharge depends on the radius of sharp point and changes with the voltage</li> <li>• Number of discharges change with applied voltage</li> <li>• Repetition rate (at 10% above the inception voltage): high</li> <li>• Inception voltage is higher than negative corona in air</li> </ul>
Negative corona in oil (measured via coupling capacitor) (4.2-b)		<ul style="list-style-type: none"> <li>• Phase of occurrence: around 270°</li> <li>• Magnitude: small</li> <li>• Repetition rate (at 10% above the inception voltage): small</li> <li>• Inception voltage is close to positive corona in oil</li> </ul>

<p>Positive corona in oil (measured via coupling capacitor) (4.2-b)</p>		<ul style="list-style-type: none"> <li>• Phase of occurrence: around 90°</li> <li>• Magnitude: high</li> <li>• Repetition rate (at 10% above the inception voltage): low</li> <li>• Inception voltage is close to negative corona in oil</li> <li>• Large positive discharges are accompanied with audible clicks</li> </ul>
<p>Surface discharge in air (measured via coupling capacitor) (4.2-c)</p>		<ul style="list-style-type: none"> <li>• Phase of occurrence: 0-90° and 180-270°</li> <li>• Magnitude: small-medium</li> <li>• PD patterns strongly depends on the geometry of the electrodes</li> <li>• Repetition rate (at 10% above the inception voltage): very high</li> </ul>
<p>Surface discharge in oil (measured via coupling capacitor) (4.2-d)</p>		<ul style="list-style-type: none"> <li>• Phase of occurrence: 330-90° and 150-270°</li> <li>• Magnitude: small-medium</li> <li>• Repetition rate (at 10% above the inception voltage): very high</li> <li>• Symmetric on both half cycles</li> </ul>
<p>Free moving bubble in oil (4.2-e)</p>		<ul style="list-style-type: none"> <li>• Phase of occurrence: almost everywhere with concentration around peaks of sinusoidal voltage</li> <li>• Magnitude: small-large</li> <li>• Magnitude depends on size of bubbles</li> <li>• Repetition rate is strongly dependent on the number of bubbles</li> <li>• Repetition rate (at 10% above the inception voltage): small</li> <li>• Symmetric on both half cycles</li> </ul>

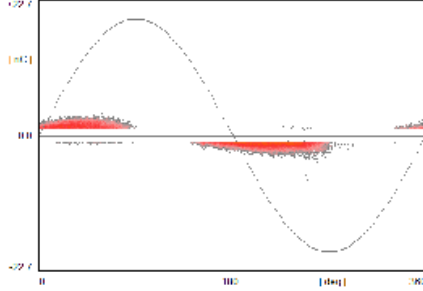
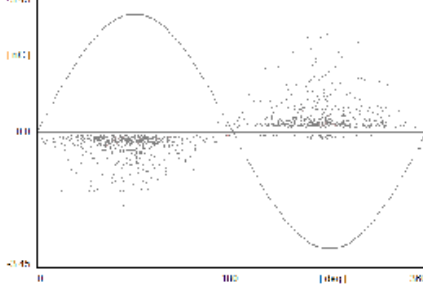
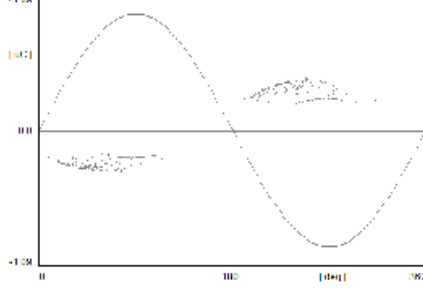
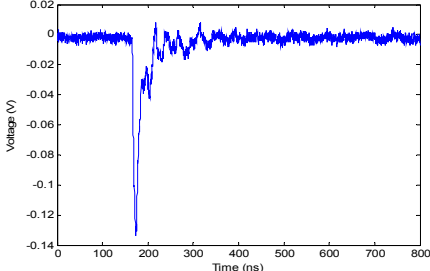
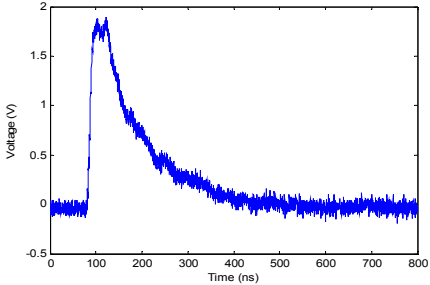
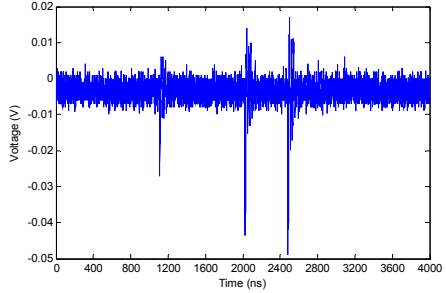
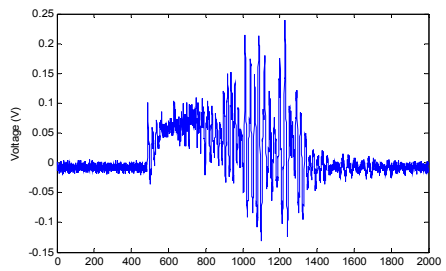
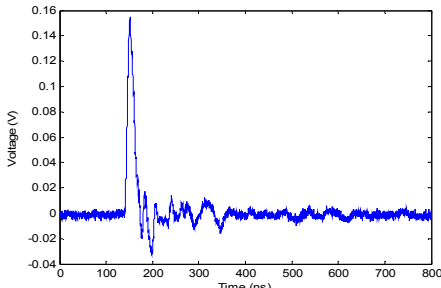
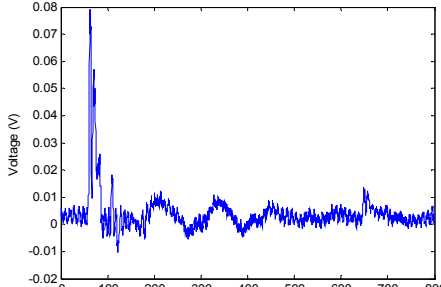
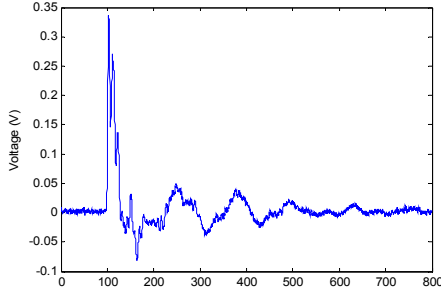
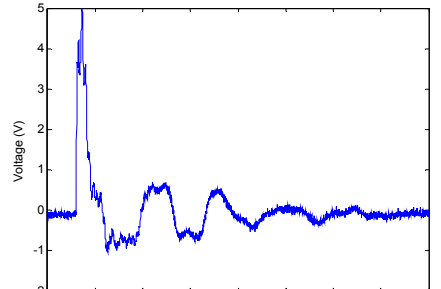
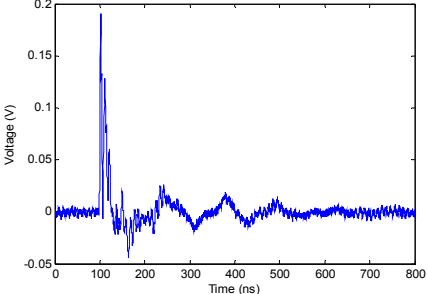
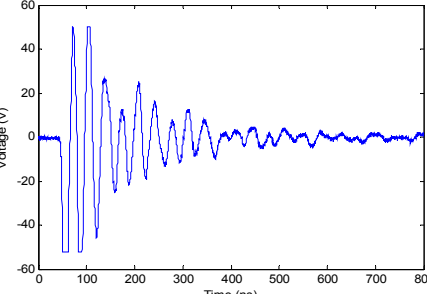
<p>Cavity between layer of paper (4.2-g)</p>		<ul style="list-style-type: none"> <li>• Phase of occurrence: 330-90° and 150-270°</li> <li>• Magnitude depends on depth of the cavity</li> <li>• Magnitude: small-large</li> <li>• Repetition rate depends on the area of cavity</li> <li>• Repetition rate (at 10% above the inception voltage): very high</li> <li>• Symmetric on both half cycles</li> </ul>
<p>metallic particle in oil (measured via coupling capacitor) (4.2-h)</p>		<ul style="list-style-type: none"> <li>• Phase of occurrence: almost everywhere on sinusoidal voltage</li> <li>• Magnitude: small-medium</li> <li>• Repetition rate (at 10% above the inception voltage): low</li> <li>• Symmetric on both half cycles</li> </ul>
<p>Metal object at floating potential (measured via coupling capacitor) (4.2-i)</p>		<ul style="list-style-type: none"> <li>• Phase of occurrence: 0-90° and 180-270°</li> <li>• Magnitude: extremely large</li> <li>• Repetition rate (at 10% above the inception voltage): low</li> <li>• Accompanied by audible clicks</li> <li>• Symmetric on both half cycles</li> </ul>

Table 4.2. PD waveform due to different defects and their corresponding characteristics

	Characteristic PD pulse shape	Characteristics
<p>Negative corona in air (4.2-a)</p>	 <p>The graph shows a single, sharp negative pulse. The y-axis is labeled 'Voltage (V)' ranging from -0.14 to 0.02. The x-axis is labeled 'Time (ns)' ranging from 0 to 800. The pulse reaches a minimum of approximately -0.13 V at about 150 ns.</p>	<ul style="list-style-type: none"> <li>• Rise time: 6 ns</li> <li>• Fall time: 37 ns</li> <li>• Pulse duration: 12 ns</li> <li>• Pulse width: 46 ns</li> </ul>
<p>Positive corona in air (4.2-a)</p>	 <p>The graph shows a broad, positive pulse. The y-axis is labeled 'Voltage (V)' ranging from -0.5 to 2. The x-axis is labeled 'Time (ns)' ranging from 0 to 800. The pulse rises to a peak of about 1.8 V at 100 ns and then decays slowly towards zero.</p>	<ul style="list-style-type: none"> <li>• Rise time: 73 ns</li> <li>• Fall time: 1072 ns</li> <li>• Pulse duration: 398 ns</li> <li>• Pulse width: 1297 ns</li> </ul>
<p>Negative corona in oil (4.2-b)</p>	 <p>The graph shows a train of sharp, negative pulses. The y-axis is labeled 'Voltage (V)' ranging from -0.05 to 0.02. The x-axis is labeled 'Time (ns)' ranging from 0 to 4000. The pulses are clustered between 1000 and 2500 ns.</p>	<ul style="list-style-type: none"> <li>• Rise time: 1 ns</li> <li>• Fall time: 5 ns</li> <li>• Pulse duration: 2 ns</li> <li>• Pulse width: 6 ns</li> <li>• Usually a pulse train occurs at the same time</li> <li>• The magnitude of the pulses starts from the smallest and ends to the largest</li> </ul>
<p>positive corona in oil (4.2-b)</p>	 <p>The graph shows a complex, oscillating positive pulse. The y-axis is labeled 'Voltage (V)' ranging from -0.15 to 0.25. The x-axis is labeled 'Time (ns)' ranging from 0 to 2000. The pulse starts around 400 ns and exhibits multiple peaks and troughs between 600 and 1400 ns.</p>	<ul style="list-style-type: none"> <li>• Rise time: 260 ns</li> <li>• Fall time: 600 ns</li> <li>• Pulse duration: 360 ns</li> <li>• Pulse width: 880 ns</li> </ul>

<p>Surface discharge in air (4.2-c)</p>		<ul style="list-style-type: none"> <li>• Rise time: 7 ns</li> <li>• Fall time: 16 ns</li> <li>• Pulse duration: 16 ns</li> <li>• Pulse width: 27 ns</li> </ul>
<p>Surface discharge in oil (4.2-d)</p>		<ul style="list-style-type: none"> <li>• Rise time: 3 ns</li> <li>• Fall time: 21 ns</li> <li>• Pulse duration: 15 ns</li> <li>• Pulse width: 26 ns</li> </ul>
<p>Free moving bubble in oil (4.2-e)</p>		<ul style="list-style-type: none"> <li>• Rise time: 3 ns</li> <li>• Fall time: 22 ns</li> <li>• Pulse duration: 14 ns</li> <li>• Pulse width: 27 ns</li> </ul>
<p>Cavity between layer of paper (4.2-g)</p>		<ul style="list-style-type: none"> <li>• Rise time: 10 ns</li> <li>• Fall time: 17 ns</li> <li>• Pulse duration: 21 ns</li> <li>• Pulse width: 31 ns</li> </ul>

<p>Metallic particle in oil (4.2-h)</p>		<ul style="list-style-type: none"> <li>• Rise time: 2 ns</li> <li>• Fall time: 21 ns</li> <li>• Pulse duration: 11 ns</li> <li>• Pulse width: 25 ns</li> </ul>
<p>Metal object at floating potential (4.2-i)</p>		<ul style="list-style-type: none"> <li>• Rise time: 4 ns</li> <li>• Fall time: 4 ns</li> <li>• Pulse duration: 43 ns</li> <li>• Pulse width: 15 ns</li> </ul>

#### 4.4 PD measurement on a 36 kV bushing

An in-service aged 36 kV oil impregnated paper transformer bushing, type GOH 170/25 which has PD activity was investigated as attempt to identify the type of PD. Figure 4.4 shows a photo of the bushing. Acquired PD patterns were measured at different voltage levels. Figure 4.5 shows the PD pattern with different voltage level applied to the bushing. Figure 4.6 shows different types of PD waveform recorded from the bushing tap.



Figure 4.4: A photo of a transformer bushing; type 170/25 GOH



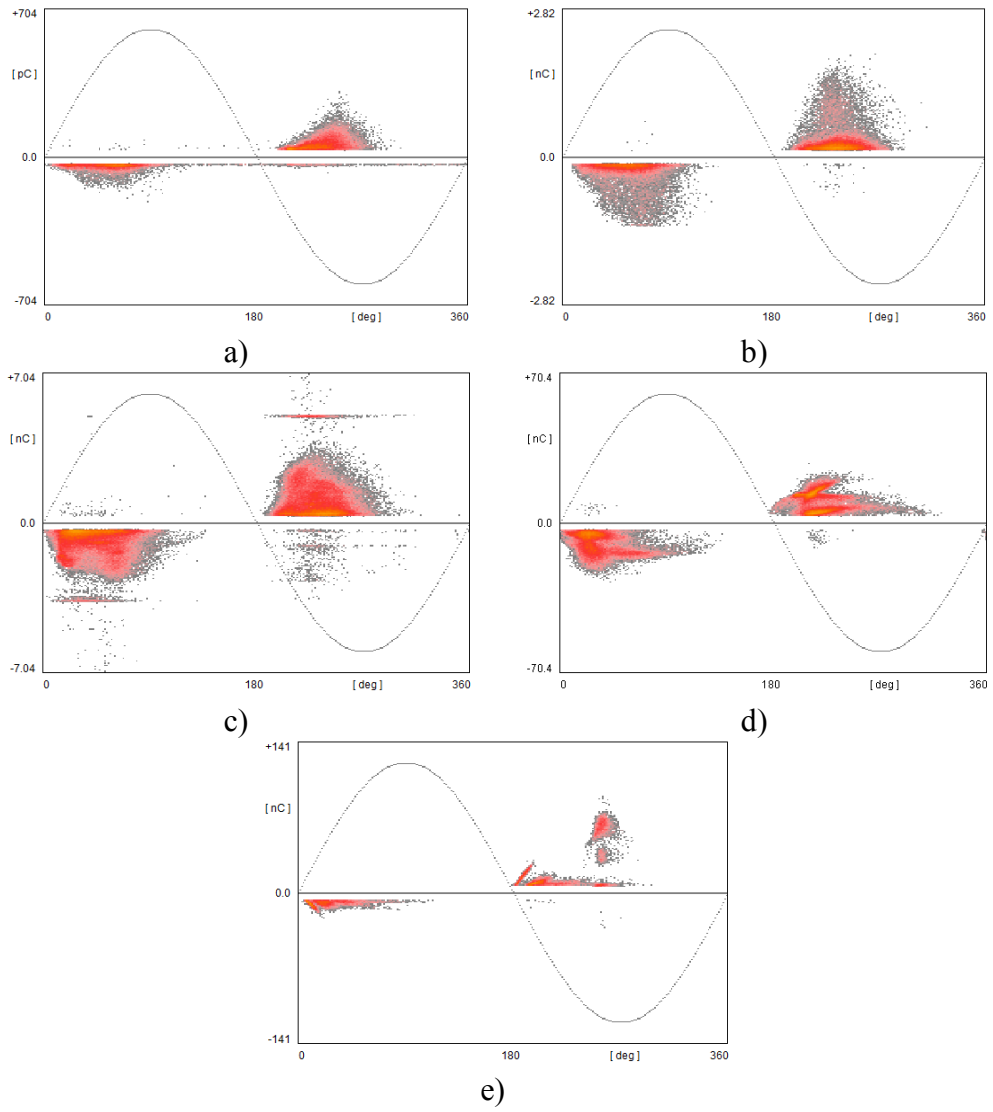


Figure 4.5: PD patterns measured on a 36 kV aged bushing. Applied voltage:  
a) 19 kV, b) 22 kV, c) 25 kV, d) 28 kV, e) 35 kV

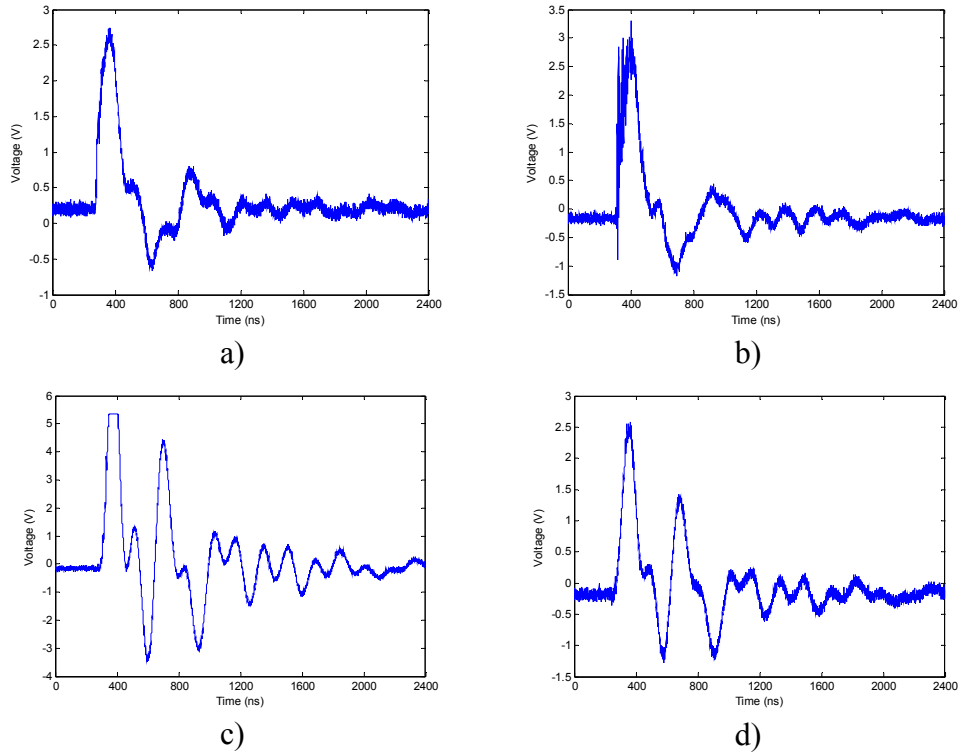


Figure 4.6: PD waveforms recorded from the 36 kV aged bushing at 35 kV

By comparing figure 4.5 to the patterns in table 4.1 it is clear that the PD pattern can only be for surface discharge in oil or for void discharge. However according to figure 4.5-d which shows the well-known rabbit-ear on the pattern it is clear that the pattern is due to void discharge. At higher voltage another spot appears around the phase of  $270^\circ$  which is a sign of negative corona in air. After inspection it became clear that these PDs are due to a ground wire which passed close to the high voltage side of the bushing.

According to the PD waveform detected by the oscilloscope it is also clear that there are four kinds of discharge. However the PD waveforms in the figure 4.6-a and figure 4.6-b are actually very similar which means they are from the same site and same source. However one of them is related to the main part of the void PD pattern and another one is related to the ear part of the void PD pattern. As is also clear in figure 4.6-d, the PD pattern which is related to void discharge has a rabbit ear. It is why the

waveform on figure 4.6-a and figure 4.6-b are a little different. The same thing also is valid for figure 4.6-c and figure 4.6-d. They are actually the same waveform with different magnitude which corresponds to negative corona in air. This is also visible in figure 4.5-e where part of the pattern shows two spots around the phase of  $270^\circ$ .



## Chapter 5

### Disturbing sources of PD

Four types of disturbances which are actually PD, but most likely occur outside a transformer, are shortly explained in this chapter.

#### 5.1 Corona in air

Corona is important mainly because of corona loss in transmission line. However corona in high voltage equipment could be a source of disturbance during PD measurement.

In a substation, where the power transformer is located, there are many kinds of disturbance from the environment. One of the most important disturbances is due to the PD pulses from corona. Corona could occur on the high voltage overhead line or wherever there is a sharp bare conductor connected to high enough voltage. During an on-line PD measurement it is important to remove all the noise from the measured signals to be sure that what is measured is due to harmful PD inside the transformer. From this respect the study of corona in air has some degree of importance.

To simulate corona in air a point-hemisphere electrode is used. The diameter of the hemisphere is 100 mm and the gap between the point electrode and the hemisphere is adjustable. The point electrode's curvature is 0.2 mm and the gap distance is fixed at 25 mm. By applying a high voltage to the point electrode and connecting the hemisphere to ground corona in air can be observed. For this configuration at low voltage, corona only occurs in the negative half cycle and it occurs symmetrically around the negative peak of the sinusoidal voltage. By increasing the applied voltage, positive corona appears around the positive peak. The magnitude of positive corona is much higher than negative corona, for instance in this experiment negative corona is in the order of 150 pC while positive corona is about 5 nC.

A little above the corona inception voltage only a few corona pulses are observed. By increasing the applied voltage further, the number of corona discharges increases but their magnitude remains constant. If the voltage increases more, the corona

magnitude also changes slightly. Figure 5.1 shows corona patterns at 6 kV and at 13 kV. Figure 5.2 shows a positive corona at 18 kV.

If the high voltage is connected to the hemisphere and the point electrode is grounded, corona occurs sooner in the positive half cycle. By increasing the applied voltage further, big corona pulses occur in the negative half cycle.

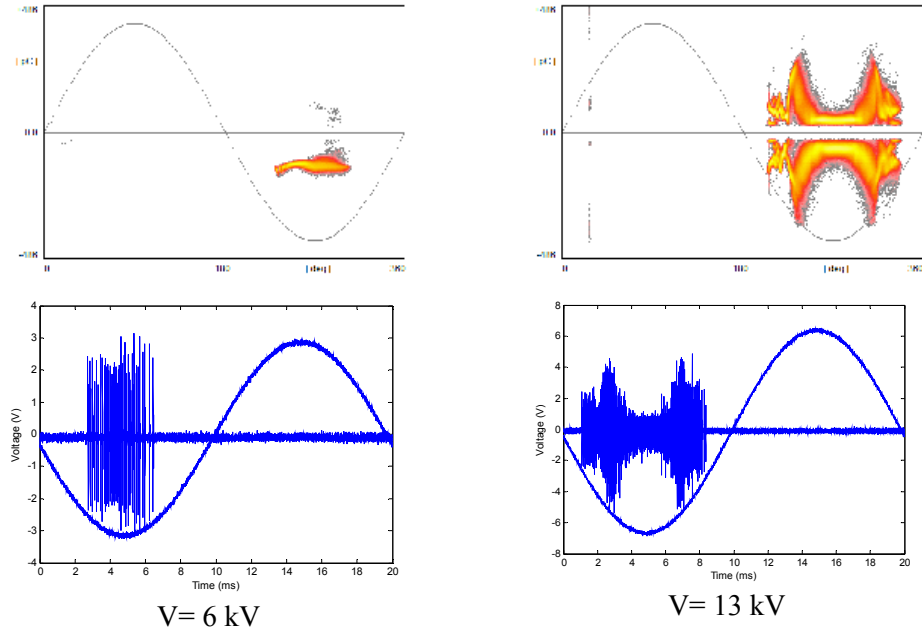


Figure 5.1: Negative corona at 6 kV and 13 kV (corona inception voltage: 4.8 kV)

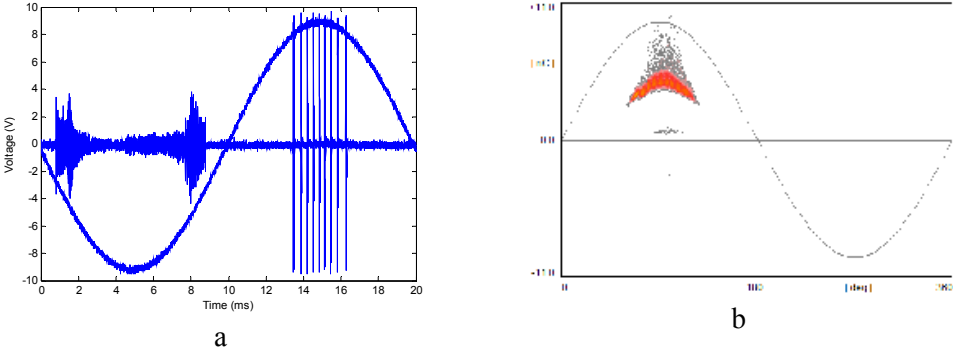


Figure 5.2: Positive corona at 18 kV, PDIV is 16 kV, note: amplifier is saturated for the left figure and that is why the magnitude of positive corona is comparable with negative corona.

The inception voltage of corona depends mainly on the curvature of the point and the distance between the high voltage electrode and ground. The electric field near a point in a point-plane electrode can be obtained by equation 5.1[6]:

$$E_{max} = \frac{2V}{R \ln\left(\frac{4H}{R}\right)} \quad (5.1)$$

In equation 5.1,  $E_{max}$  is the electric field next to the point,  $V$  is the applied voltage,  $R$  is radius of curvature of the needle tip and  $H$  is distance between the point and the ground electrode. Corona inception electric field  $E_i$ , valid for air at normal temperature and pressure (NTP), can be calculated by equation 5.2 [11]:

$$E_i = E_0(1 + 4 \cdot 10^{-3}H) \left[ 1 + \frac{0.166}{R_e^{0.45}} \right] \quad (5.2)$$

In equation 2,  $E_0 = 2.38$  MV/m and  $H =$  absolute humidity in g/m<sup>3</sup>

Corona inception voltage  $V_0$  can be calculated by equation 5.3 [11]:

$$V_0 = E_i R_e$$

$$R_e = 0.5 \ln(1 + 2d/R) \quad (5.3)$$

In equation 5.3,  $d$  is gap distance and  $R$  is the point electrode curvature [11].

## 5.2 Surface discharge in air

Surface discharge in air may appear on the surface of a transformer bushing. It is also important to distinguish this kind of discharge from those partial discharges that occur inside. In order to simulate surface discharge on mica insulation, a small insulator which is made of porcelain is used as shown in figure 5.3.



Figure 5.3: Test setup for surface discharge in air

In order to have surface discharges at lower voltages, a piece of copper foil is wrapped around the middle of the insulator. The PD pattern for surface discharge in air is shown in figure 5.4-a. The PD pattern is not symmetric and it has higher value in the negative voltage polarity. This is because the copper foil with a sharp edge is connected to ground. If the high voltage is connected to the copper foil and the top of the insulator is grounded then higher values of PD activity are observed in the positive polarity as shown in figure 5.4-b.

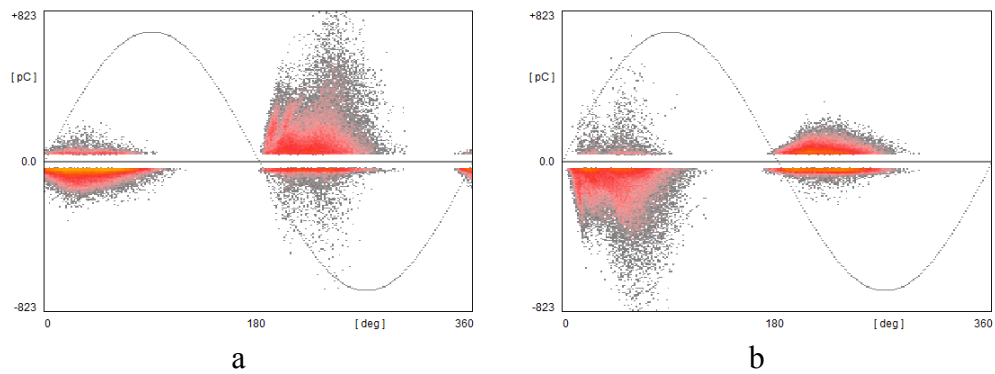


Figure 5.4: Surface discharge pattern on the surface of a mica insulator. a) high voltage connected to the top electrode, b) high voltage connected to a copper foil with sharp edge

### 5.3 Ungrounded metal near to measurement system

Any ungrounded conductive object close to the high voltage could have concentrations of field around its edges and if the electric field is sufficiently large it can produce a discharge. These discharge pulses are capacitively coupled to the PD measurement circuit and may lead to misinterpretation of the results. If there are



unusual PD patterns on the measurement results it is suggested to use an ultrasonic PD detector in order to detect any external PD source. The PD pattern due to an unearthed conductive object depends very much on the structure and position of the object. Figure 5.5 shows two PD patterns due to an unearthed metallic wire close to the oil chamber.

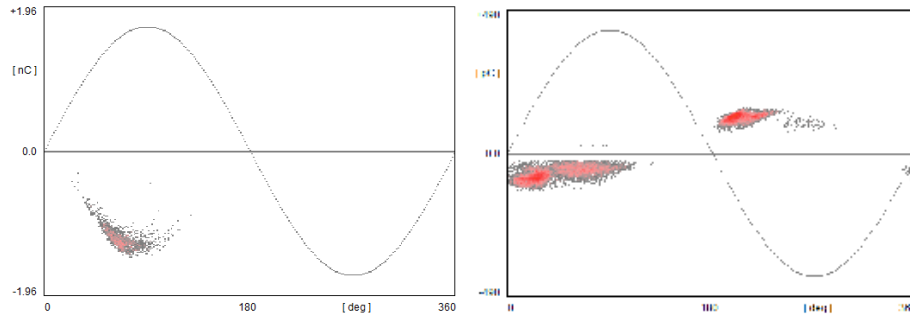


Figure 5.5: Two PD patterns corresponding to unearthed metallic object close to the experimental setup

#### 5.4 Ungrounded bushings tap

The outermost foil of a transformer bushing is usually connected to the bushing tap and this tap can be used for the purpose of diagnostics. Normally the bushing tap is short circuited to ground. However, if by mistake it is not connected to ground then it can generate a lot of PDs. Figure 4.6 is an example where the bushing tap was not connected to ground.

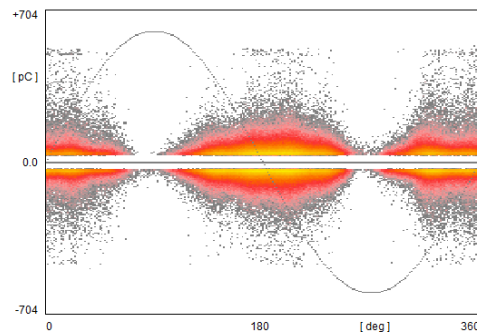


Figure 5.6: PD patterns due to ungrounded bushing tap



## Chapter 6

### Effect of temperature on partial discharge

In most solid insulators, as the temperature goes up the dielectric losses increase and cause the insulation temperature to increase further. Usually an increase in temperature results in a decrease of the resistivity of the insulation which results in more current passing through the insulation. This process may enhance itself and lead to current run-away and ultimately breakdown in the insulation [44].

The case is different for transformer oil. Many experiments performed on transformer oil show that an increase of oil temperature within the normal range increases the oil breakdown strength. An increase of the oil temperature increases the mobility of charge carriers, and therefore the conductivity of the oil increases which could result in reduction of oil breakdown strength. However it is clear that the above explanation doesn't fit the measurement result so there must be another dominant mechanism. There are two possible explanations to this observation which are necessary to be mentioned. The first assumption is related to the amount of moisture in oil. As the oil temperature increases, the amount of moisture in the oil decreases and this could be the reason why the breakdown strength of oil increases with increasing temperature. A second possible explanation is that there is an amount of dissolved gas in oil. The solubility of gas increases with the increase of temperature and that could explain why the breakdown strength of oil is higher for higher temperatures [50].

Not only can temperature affect the oil breakdown strength, but also it can affect the PD activity inside a transformer. Investigation of the change in PD activity due to an increase of temperature not only makes the laboratory results closer to reality but also it can be used as a factor for classification. For example, if during overload conditions the PD activity decreases then it can be a good indicator to identify the kind of defect that is the source of the discharges. In figures 6.1 -6.4, PD inception voltage as a function of temperature is shown for four kinds of defects in an oil filled transformer. As is clear from figures 6.1 -6.4, the PD inception voltage for corona in oil and a metallic object at floating potential increases with the increase of temperature, but for surface discharge in oil and free bubble in oil the PD inception voltage decreases with the increase of temperature.

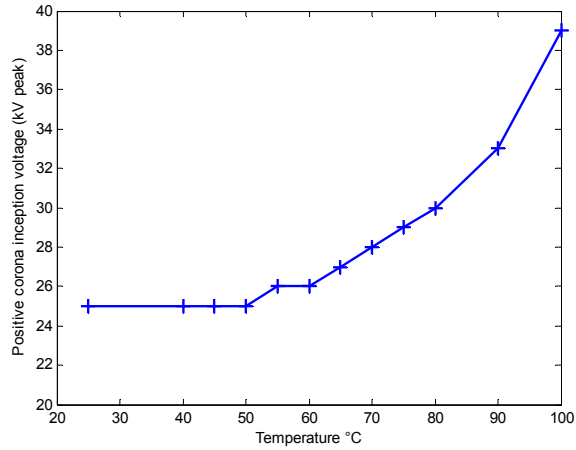


Figure 6.1: Corona (in oil) inception voltage versus temperature

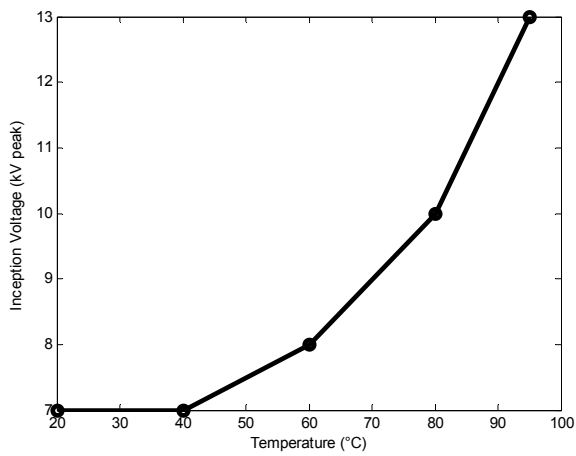


Figure 6.2: Metal object at floating potential (PD inception voltage versus temperature)

For the case of corona in oil, since the gradient of the electric field near to the sharp point is high it forces the particles in oil to move towards the sharp point. When the temperature is high the conductive particles in oil can move easier and faster toward the needle tip and they moderate the electric field around the needle tip. This is the reason why at high temperature the corona inception voltage is higher.

For the case of a metallic object at floating potential the discharge is some sort of complete breakdown that occurs in the oil gap between the electrode and the metal

object. As a result the behavior of this kind of discharge versus temperature is similar to the behavior of oil breakdown versus temperature.

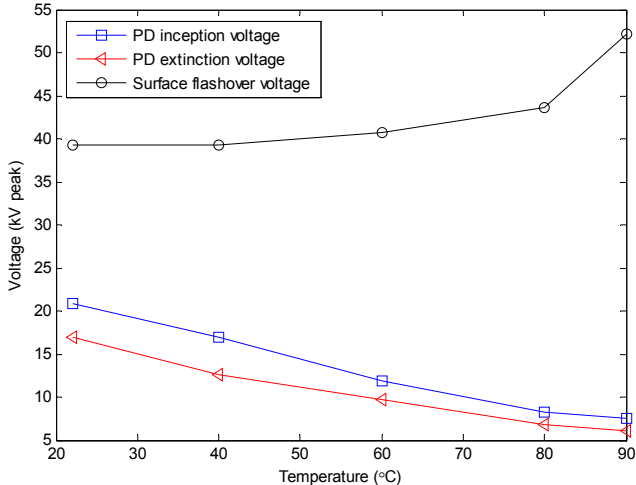


Figure 6.3: Surface discharge in oil: PD inception voltage as a function of temperature

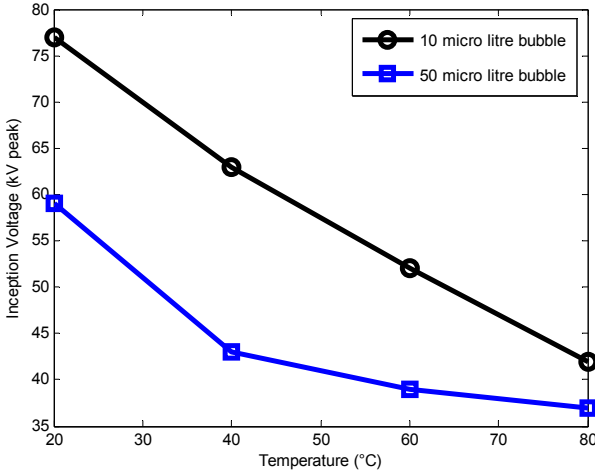


Figure 6.4: Air bubble in oil adjacent to pressboard surface (PD inception voltage as a function of temperature)

For the case of surface discharge in oil there are two phenomena. One is surface discharges and the other is surface flashover. The inception voltage for surface flashover increases as the temperature increases. Again this is related to oil

breakdown strength, since the flashover has to occur in the oil phase. This means a kind of breakdown in oil phase which has already been discussed, and as temperature increases the breakdown strength also increase. However for the PD inception voltage the case is different. In this case since the needle tip is connected to the pressboard surface, the pressboard also affects the inception voltage. For higher temperatures the electron release from the charge-traps on the pressboard surface is easier. This means that the availability of the initial seed electron that is needed for streamer initiation is higher for higher temperature. This is why surface discharge inception voltage decreases with increase of temperature.

For the case of a bubble in oil, the bubble which leans to pressboard layer is not spherical. This means that the bubble is in the ellipse shape with the larger diameter is parallel to the pressboard surface. For higher temperature the oil surface tension decreases which results in the bubble diameter (big diameter) becoming larger. When the sinusoidal voltage is crossing zero there is zero voltage drop on the gas bubble in oil. As long as the applied voltage increases the voltage drop on the bubble also increases. At the same time due to dielectrophoretic force the bubble elongates in the direction of electric field. This means that the air gap needed for breakdown will be higher than before. The voltage keeps raising and so the voltage drop on the bubble until when the voltage drop is enough to make a discharge inside the bubble. The resultant of the initial elongation (parallel to the pressboard layer) and later elongation (perpendicular to pressboard layer, due to the electric field) is in such way that for higher temperature the final bubble shape is flatter. It is clear that a flat bubble causes a higher field-enhancement than a spherical bubble, so the partial discharge inception voltage decreases with the increase of temperature.

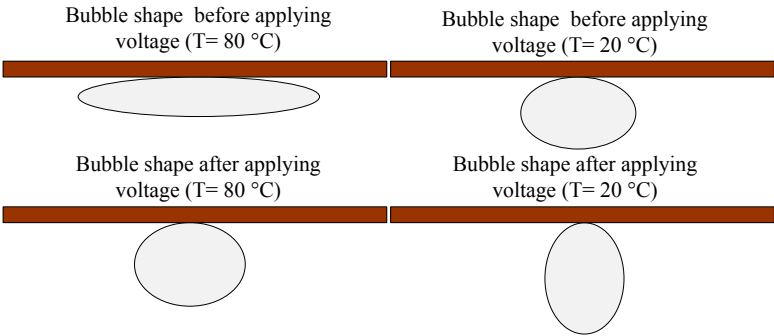


Figure 6.5: Variation of bubble geometry dependent to temperature and applied voltage

## Chapter 7

### **Deterioration of oil-impregnated paper due to PD activity**

Continuous activity of partial discharges in a void inside solid insulation or on the surface of the insulation deteriorates the insulation, and it could finally lead to breakdown. During the occurrence of partial discharges, electrons and positive and negative ions with enough energy can break the chemical bonds of the insulation. Discharge byproducts such as ozone or nitric acid can enhance the deterioration process. Apart from the deterioration mechanism, the consequence of deterioration is a reduction of the breakdown strength of solid insulation [35, 42].

In order to understand the deterioration process of oil impregnated paper which is the main insulation for oil filled transformers, a number of experiments were performed on a test object including a cavity between layers of paper.

The results from the experiments show that for a cavity embedded between layers of paper the repetition rate and the maximum magnitude of the PD (of the phase 0 degrees) increase at the initial stage of ageing and finally reach a peak value. After they reach a peak value they start to decrease slowly over time, and finally breakdown occurs on the insulation. The change of PD pattern over time for a test sample is shown in figure 7.1. The test sample includes 4 layers of oil-impregnated papers. A disc shaped cavity was punched on 2 layers of these papers. Complete details about the study are given in paper IV.

Figure 7.2 shows the corresponding PD parameter obtained from the experiment. PD repetition rate and maximum magnitude of PD (around phase 0 degree) is shown in figure 7.2. The results show that during continuous online PD monitoring, even if the PD magnitude or repetition rate does not increase, it does not mean that the insulation system is in trustable condition.

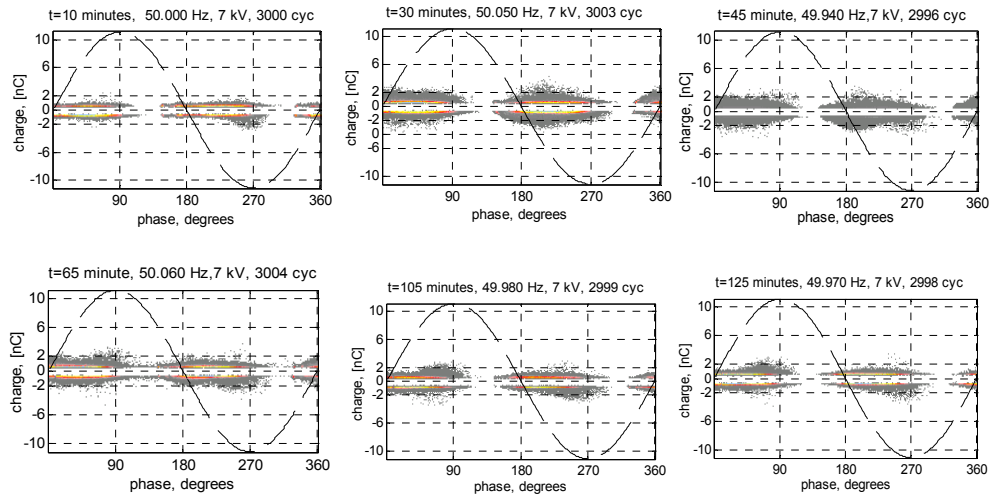


Figure 7.1: PD patterns acquired for 1 minute at 10, 30, 45, 65, 105 and 125 minutes after the first the voltage application

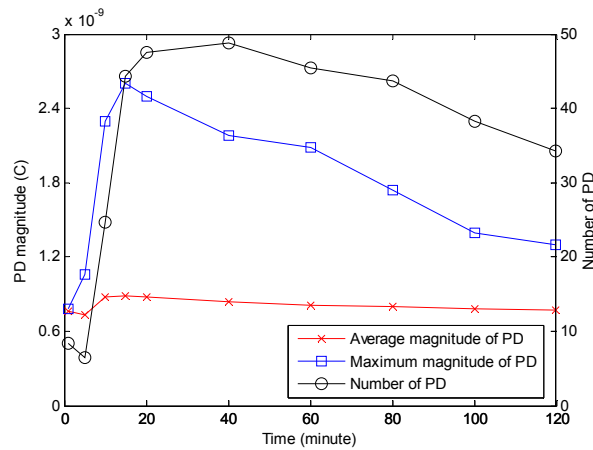


Figure 7.2: Maximum PD magnitude, Average PD magnitude and Number of PD (per 50 Hz cycle) at positive half cycle recorded for duration of one minute at different times before breakdown

In order to explain the behavior of these curves a set of experiments were conducted. Two new identical samples (sample 1 and sample 2) were prepared in order to investigate the effect of moisture. The void's diameter was larger (12 mm) in order to better highlight any changes. Dielectric spectroscopy of both samples was measured



at first. Sample 1 was left in ambient conditions in the laboratory and sample 2 was placed under voltage and PD activity. After 24 hours, the frequency dielectric response was measured for both of them. Both frequency responses had a shift but the shift related to the sample exposed to PD activity (sample 2) was much bigger. These two samples were left under ambient conditions in the lab for another 5 days. The dielectric spectroscopy after 5 days showed a shift again for both samples. However the shift in sample 1 was larger than in sample 2. Figure 7.3 and figure 7.4 shows the shift due to PD activity and exposure to ambient condition over time for real and imaginary parts respectively. In order to explain this behavior one should consider the origin of the moisture. One source of moisture is possibly the PD activity that may break the bonds of cellulose; moisture would appear as a byproduct of this activity. Another source of moisture is the environment. Possibly the shift in dielectric response is due to  $(OH)^-$  and  $(H_3O)^+$  which may come from either self-dissociation of water or from bond-scission by the PD along the cellulose molecules.

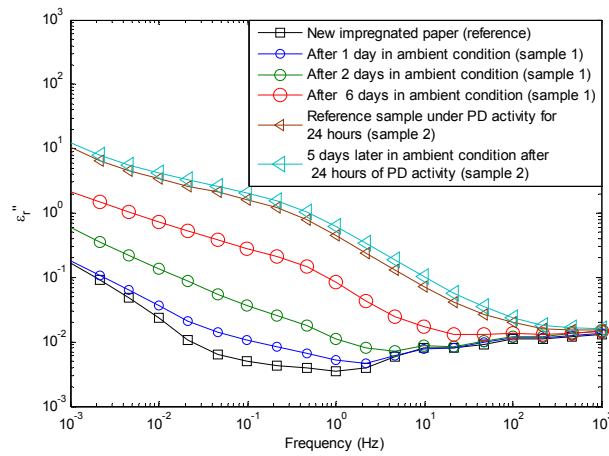


Figure 7.3: Changing of  $\epsilon''_r$  due to the effect of PD activity and exposure to ambient conditions

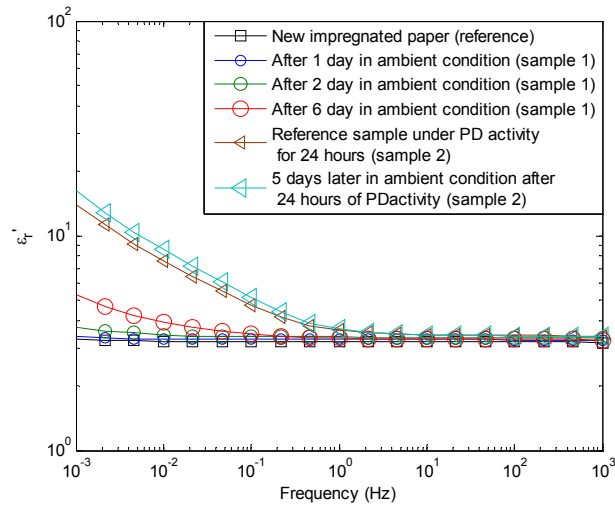


Figure 7.4: Changing of  $\epsilon_r''$  due to effect of PD activity and exposure to ambient conditions

An extrapolation of the lifetime in the presence of PD activity in a cavity between layers of paper is given in figure 7.5.

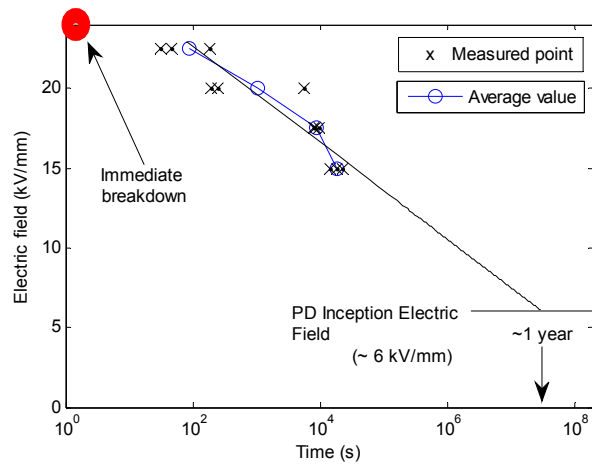


Figure 7.5: Voltage life as a function of stress, for a sample with 4 layers of unaged paper of which 2 layers have a cavity with 3 mm diameter. The solid black line is the extrapolation

## **Chapter 8**

### **Summary of publications**

#### **Paper I**

In this paper corona discharge in oil from a needle-plate geometry was investigated both in time domain, and by means of PD patterns. Positive and negative corona patterns and their waveforms in the time domain show that they are fully distinguishable from each other. The effect of geometry of the test setup such as the needle length and the gap distance between the needle-tip and ground electrode on the corona inception voltage was investigated. It was shown that only the electric field near the needle-tip is responsible for corona initiation and it is possible to predict the corona inception voltage for different gap lengths as long as one has a reference point. The effect of temperature on corona in oil shows that increasing the temperature increases the corona inception voltage and decreases corona repetition rate. Experimental results show that increasing the amount of humidity in oil decreases the corona inception voltage slightly and increases the repetition rate of corona drastically.

#### **Paper II**

In this paper partial discharge due to air bubbles in oil was investigated. Two cases were investigated; free moving bubbles, and a bubble adjacent to pressboard. In the case of moving bubbles the results show that PD patterns are symmetric around the peak of the sinusoidal voltage on both polarities. In the case of a bubble adjacent to the pressboard it was observed that when PD occur the air bubbles explode and convert to smaller bubbles. The results showed that the inception voltage for smaller bubbles is higher than for larger bubbles and therefore the PD activity stops soon after the occurrence of the first PD. The experimental results for the inception voltage and what was calculated from Paschen's curve did not match well. This difference was explained by the fact that bubbles were elongated under electrical field and their geometry changed in comparison to what was considered in the calculation.

### **Paper III**

This paper is a continuation of the second paper. In the case of free moving bubbles, water vapor bubbles were used instead of air bubbles. The PD Pattern shows similar behavior to moving air bubbles. The PD pattern due to a cavity between layers of pressboard has been recorded. The comparison of PD patterns between free bubbles in oil and a cavity inside a solid insulation shows a clear difference which is useful for PD classification purpose. The paper also discussed the PD pattern due to a metal object at floating potential. The results showed that PD pattern in this case is symmetric in both polarities. The effect of temperature on PD behavior for a metal object at floating potential showed that the inception voltage for a metal object at floating potential increase with increasing temperature. However, an increase in temperature resulted in a decrease of inception voltage for the case of bubble in oil.

### **Paper IV**

In this paper surface discharge on the oil-pressboard interface was investigated. The effect of temperature from 20 °C to 90 °C on surface discharge inception, extinction and surface flashover voltage was investigated. Recorded PD pulses in the time domain showed that they are a combination of two kinds of PD, one of them being positive corona pulses and another surface discharge pulses. The results showed that PD inception and extinction voltages decrease with an increase in temperature while the surface flashover voltage increases. The results show that the number and the maximum magnitude of PD increase over time, but for 90 °C they reach a stable value after few hours of PD activity. It was observed that after each surface flashover the number and maximum magnitude of PD decreases immediately and it grow slowly again after that. Generally, carbon deposit on the surface of the pressboard after few hours of PD activity is higher when the temperature is higher.

### **Paper V**

In this paper, the effect of high voltage impulses on PD pattern due to a cavity between layers of paper was investigated. Three studies were performed. In the first study the test sample was aged by elevated AC voltage up to 5 hours. In the second study, the test sample was stressed by four high voltage impulses, whereas in the third study the test sample was aged at elevated AC voltage for 5 hours, but with four high voltage impulses injected at selected times during the experiment. The results showed that high voltage impulses could have a large impact on the behavior of PD

patterns if the test sample is aged by partial discharges, but a smaller effect when the test sample is unaged. The results from dielectric spectroscopy showed that ageing due to PD activity affects drastically the real and imaginary parts of complex permittivity. These changes have been explained in part II of this paper.

## **Paper VI**

In this paper partial discharge activity due to a cavity between layers of paper from beginning up to final puncture breakdown was investigated. The main focus of this paper was the investigation of the effect of thermal ageing and partial discharge deterioration on parameters such as the number, maximum magnitude and average magnitude of PD. PD behavior in a cavity can be divided into three major stages. During the first stage, which has a very short duration, big PDs occur. After that the number and maximum magnitude of PD increase until they reach a peak value. Finally at the third stage, the number and maximum magnitude of PD start to decrease gradually and slowly. Most of the time when the test sample resists PD activity is during the third stage and eventually breakdown occurred in the end of the third stage. The same study has been performed on thermally aged paper. The results showed similar behavior, but the number and magnitude of PDs were higher than for unaged samples. This behavior was explained by dielectric spectroscopy measurements performed on the samples. Also one part of the paper investigated the effect of the cavity's geometry on the number and magnitude of discharges. The results showed that the longer the cavity is in the field direction the higher the magnitude of the discharges while the larger the surface area of the cavity the more the number of PDs.



## Chapter 9

### Conclusions and future work

In this work, small scale setups which simulate different kinds of possible defects in a power transformer were developed. In order to make a data bank for PD patterns, PD measurements were performed in both phase domain and time domain. The results from the phase domain show that the phase of occurrence, repetition rate, magnitude of discharge, and symmetry of pattern could be useful for PD classification. In time domain measurements, even though the PD waveforms recorded for few kinds of defect have unique characteristics, for most of other defects the PD waveforms are similar. It was also explained that the PD waveform can change if it occurs at different location along the transformer winding. Despite the above, measurements in the time domain have the power to show how many defects or how many PD sources exist in a transformer.

Investigation of the effect of temperature on PD activity was performed for a number of defects. It was shown that an increase in temperature increases the inception voltage for corona in oil and for a metal object at floating potential. However, it reduces the inception voltage for surface discharge in oil and for free bubbles in oil. It was shown that increasing the temperature results in an increase of repetition rate for the cases of surface discharge in oil and bubble in oil, and a reduction of the repetition rate for the cases of corona in oil and metal object at floating potential.

The effect of humidity was only investigated for corona in oil and it was shown that an increase of moisture in the oil decreases the inception voltage and increases the corona repetition rate drastically.

It was shown that while PD activity in oil-impregnated paper increases the repetition rate and maximum magnitude of discharges at the beginning of the ageing test, later both curves decrease slowly over time and finally complete puncture breakdown occurs. A comparison between PD activity in new and thermally aged paper was made, and it was shown that the magnitude and number of discharges for thermally aged paper is higher than for new paper. Dielectric spectroscopy results on new and thermally aged papers showed that thermally aged paper has higher conductivity

compared to new paper, which can explain why PD magnitude and PD repetition rate are different for new paper and thermally aged papers. Also result from dielectric spectroscopy on new aged samples with PD activity showed a big shift in real and imaginary parts of the frequency spectrum.

As future work it is planned to run PD measurements on a real power transformer. The PD pattern recorded from the real transformer should be analyzed in order to find the PD sources. Pressboard ageing due to surface discharges in oil, and oil ageing due to PD activity, would be of interest. Developing a model for ageing of oil-impregnated insulation due to PD activity is the final goal of these studies.



## Bibliography

- [1] H. William, P. E. Bartley, "Analysis of Transformer Failures", International Association of Engineering Insurers 36<sup>th</sup> Annual Conference – Stockholm, 2003.
- [2] R. Jongen, P. Morshuis, J. Smit, A. Janssen and E. Gulski, "A Statistical Approach to Processing Power Transformer Failure Data", 19<sup>th</sup> International Conference on Electricity Distribution, Vienna, 21-24 May 2007.
- [3] *Service handbook for transformers-3<sup>rd</sup> edition*, published by ABB.
- [4] A. M. Emsley and G. C. Stevens, "A Reassessment of the Low Temperature Thermal Degradation of Cellulose" Sixth International Conference on Dielectrics Materials, Measurement and Application, 1992.
- [5] G. J. Pukel, H. M. Muhr, W. Lick, "Transformer diagnostics: Common used and new methods" Institute of High Voltage Engineering and System Management, Graz University of Technology.
- [6] M. Goldman, R. S. Sigmond, "Corona and Insulation", IEEE Transactions on Electrical Insulation, Vol. EI-17 No. 2, April 1982.
- [7] G.J. Rohwein, "Corona Processing of Insulating Oil", Twenty-Second International Symposium Power Modulator, 25-27 June 1996.
- [8] H. Borsi and U. Schröder, "Initiation and Formation of Partial Discharges in Mineral-based Insulating Oil", IEEE Transactions on Dielectrics and Electrical Insulation, Vol. 1, No. 3, June 1994.
- [9] M. Pompili, C. Mazzetti and R. Bartnikas, "PD Pulse Burst Characteristics of Transformer Oils", IEEE Transactions on Power Delivery, Vol. 21, No. 2, April 2006.
- [10] M. Pompili, C. Mazzetti and R. Bartnikas, "PD Pulse Burst Behavior of a Transformer Type Synthetic Organic Ester Fluid", IEEE Transactions on Dielectrics and Electrical Insulation, Vol. 15, No. 6, December 2008.
- [11] M. Pompili, C. Mazzetti and R. Bartnikas, "Partial Discharge Pulse Sequence Patterns and Cavity Development Times in Transformer Oils under ac Conditions", IEEE Transactions on Dielectrics and Electrical Insulation, Vol. 12, No. 2, April 2005.

- [12] O. Lesaint and R. Tobazeon, "Streamer Generation and Propagation in Transformer Oil under ac Divergent Field Conditions", IEEE Transactions on Electrical Insulation, Vol. 23 No. 6, December 1988.
- [13] C. E. Sölver, *Discharge Pulses in Transformer Oil at Alternating Voltage. Pulse Shape and Partial Discharge Measurements*, Technical report No. 54, PhD thesis, Chalmers University of Technology, 1975.
- [14] P. M. Mitchinson, P. L. Lewin, G. Chen and P. N. Jarman, "A new approach to the study of surface discharge on the oil-pressboard interface", IEEE International Conference on Dielectric Liquids, ICDL 2008.
- [15] H. Zainuddin, P. M. Mitchinson, P. L. Lewin, "Investigation on the Surface Discharge Phenomenon at the Oil-pressboard Interface", IEEE International Conference on Dielectric Liquids, ICDL 2011.
- [16] P. M. Mitchinson, P. L. Lewin, G. Chen and P. N. Jarman, "Tracking and Surface Discharge at the Oil-Pressboard Interface", IEEE Electrical Insulation Magazine, March/April — Vol. 26, No. 2, 2010.
- [17] J. Li, W. Si, X. Yao and Y. Li, "Partial Discharge Characteristics over Differently Aged Oil/pressboard Interfaces", IEEE Transactions on Dielectrics and Electrical Insulation Vol. 16, No. 6, December 2009.
- [18] H. Gui and Z. De-Yi, "Surface Discharge Characteristics of Impregnated Pressboard Under AC Voltage", Proceedings of the 3rd International Conference on Properties and Applications of Dielectric Materials, July 8-12, 1991 Tokyo, Japan.
- [19] Y. Cheng, E. Gockenbach, C. Eichler and C. Li, "The Partial Discharge Phenomena on the Surface of Oil Impregnated Paper with Parallel Electric Field", Annual Report Conference on Electrical Insulation and Dielectric Phenomena, 2010.
- [20] W. Hui, L. Cheng-rong, S. Kang, and M. Yinyin, "Experimental Study on the Evolution of Surface Discharge for Oil-Paper Insulation in Transformers", Annual Report Conference on Electrical Insulation and Dielectric Phenomena, 2009.
- [21] H. Wang and C. Li, "Influence of Temperature to Developing Processes of Surface Discharges in Oil-Paper Insulation", IEEE International Symposium on Electrical Insulation (ISEI), 6-9 June 2010.
- [22] ABB Product Group Insulation & Components, "Bubble Evolution in Bushings", Product guide, No. 1ZSC000001C2704, 2011-05-04.

- [23] T. V. Oommen, S. R. Lindgren, "Bubble Evolution from Transformer Overload", IEEE Transmission and Distribution Conference and Exposition, 2001
- [24] H. Shiota, H. Muto, H. Fujii and N. Hosokawa, "Diagnosis for Oil-Immersed Insulation Using Partial Discharge Due to Bubbles in Oil", 7th International Conference on Properties and Application of Dielectric Materials, June 1-5 2003 Nagoya.
- [25] X. Chen, A. Cavallini, G. C. Montanari, "Improving High Voltage Transformer Reliability through Recognition of PD in Paper/Oil Systems", International Conference on High Voltage Engineering and Application, Chongqing, China, November 9-13, 2008.
- [26] K. X. Lai, B. T. Phung, T. R. Blackburn, "Investigation of Partial Discharge in Single Void and Multi-Void Using Data Mining", Power Engineering Conference, AUPEC 2009.
- [27] C. Forssén, *Modelling of cavity partial discharges at variable applied frequency*. Ph.D. thesis, Kungl Tekniska Högskolan (KTH), Stockholm, May 2008.
- [28] S. I. Cho, "*On-Line PD (Partial Discharge) Monitoring of Power system Components*", Master of Science in Technology thesis, School of Electrical engineering, Aalto University 2011.
- [29] H. G. Kranz, "Diagnosis of Partial Discharge Signals using Neural Networks and Minimum Distance Classification", IEEE Transactions on Electrical Insulation Vol. 28 No. 6, December 1993.
- [30] F. H. Kreuger, E. Gulski and A. Krivda, "Classification of Partial Discharges", IEEE Transactions on Electrical Insulation Vol. 28 No. 6, December 1993.
- [31] T. Brosche, W. Hiller, E. Fauser, "Novel Characterization of PD Signals by Real-time Measurement of Pulse Parameters", IEEE Transactions on Dielectrics and Electrical Insulation Vol. 6 No. 1, February 1999.
- [32] S. D. R. Suresh, S. Usa, "Cluster Classification of Partial Discharges in Oil impregnated Paper Insulation", Advances in Electrical and Computer Engineering, Volume 10, Number 1, 2010.
- [33] S. M. Strachan, S. Rudd, S. D. J. McArthur, M. D. Judd, S. Meijer and E. Gulski, "Knowledge-Based Diagnosis of Partial Discharges in Power Transformers", IEEE Transactions on Dielectrics and Electrical Insulation Vol. 15, No. 1, February 2008

- [34] N. C. Sahoo, M. M. A. Salama, "Trends in Partial Discharge Pattern Classification: A Survey", IEEE Transactions on Dielectrics and Electrical Insulation Vol. 12, No. 2; April 2005
- [35] F. H. Kreuger. *Discharge detection in high voltage equipment*. Temple Press Books Ltd, London, 1964.
- [36] P. H. F. Morshuis, "Degradation of Solid Dielectrics due to Internal Partial Discharge: Some thoughts on progress made and where to go now", IEEE Transactions on Dielectrics and Electrical Insulation, Vol. 12, No. 5, October 2005.
- [37] A. Cavallini, G. C. Montanari, F. Ciani, "Analysis of Partial Discharge Phenomena in Paper-Oil Insulation Systems as a Basis for Risk Assessment Evaluation", IEEE International Conference on Dielectric Liquids, August 2005.
- [38] X. Chen, P. H. F. Morshuis, Q. Zhuang, J. J. Smit and Z. Xu, "Ageing of Oil-impregnated Transformer Insulation Studied through Partial Discharge Analysis", 2010 International Conference on Solid Dielectrics, Potsdam, Germany, July 4-9, 2010.
- [39] J. Li, W. Si, X. Yao and Y. Li, "Partial Discharge Characteristics over Differently Aged Oil/pressboard Interfaces", IEEE Transactions on Dielectrics and Electrical Insulation Vol. 16, No. 6; December 2009.
- [40] S. Okabe, G. Ueta, "Partial Discharge-induced Degradation Characteristics of Insulating Structure Constituting Oil-immersed Power Transformers", IEEE Transactions on Dielectrics and Electrical Insulation Vol. 17, No. 5, October 2010.
- [41] N. Taylor. *Dielectric Response and Partial Discharge Measurements on Stator Insulation at Varied Low Frequency*. PhD thesis, Royal Institute of Technology (KTH), Sep 2010. TRITA-EE 2010:037.
- [42] E. Kuffel, W. S. Zaengl and J. Kuffel, *High Voltage Engineering Fundamental*. Newnes, Elsevier Butterworth-Heinemann, 2nd ed., 2000.
- [43] P. Janus. *Acoustic Emission Properties of Partial Discharges in the Time-Domain and Their Application*. Master of Science Thesis Stockholm, Sweden 2012.
- [44] G. F. C. Veloso, L. E. Borges da Silva, G. Lambert-Torres, and J. O. P. Pinto, "Localization of Partial Discharges in Transformers by the Analysis of the Acoustic Emission", IEEE ISIE 2006, July 9-12, 2006, Montreal, Quebec, Canada.

- [45] J. Fuhr, "Procedure for Identification and Localization of Dangerous PD Sources in Power Transformers" IEEE Transactions on Dielectrics and Electrical Insulation Vol. 12, No. 5; October 2005
- [46] A. Mazhab Jafari, A. Akbari, H.R. Mirzaei, M. Kharezi and M. Allahbakhshi, "Investigating Practical Experiments of Partial Discharge Localization in Transformers using Winding Modeling", IEEE Transactions on Dielectrics and Electrical Insulation Vol. 15, No. 4, August 2008.
- [47] A. Akbari, P. Werle, H. Borsi and E. Gockenbach, "Transfer-Function-Based Partial Discharge Localization in Power Transformers: A Feasibility Study", Electrical Insulation Magazine, IEEE, September/October 2002, Vol. 18, No. 5.
- [48] Power Diagnostix Systems GmbH, Bruesseler Ring 95a, 52074 Aachen, Germany ([www.power-diagnostix.com](http://www.power-diagnostix.com), last visited March 2012).
- [49] H. Edin. *Partial Discharges Studied with Variable Frequency of the Applied Voltage*. PhD thesis, Royal Institute of Technology (KTH), Sep 2001. TRITA-EEK-0102.
- [50] S. V. Kulkarni and S .A. Khaparde. *Transformer Engineering Design and Practice*. Marcel Dekker, INC.